

# A Class Inference Scheme With Dempster-Shafer Theory for Learning Fuzzy-Classifier Systems

HIROKI SHIRAIISHI, Yokohama National University, Japan

HISAO ISHIBUCHI\*, Southern University of Science and Technology, China

MASAYA NAKATA\*, Yokohama National University, Japan

The decision-making process significantly influences the predictions of machine learning models. This is especially important in rule-based systems such as Learning Fuzzy-Classifier Systems (LFCSs) where the selection and application of rules directly determine prediction accuracy and reliability. LFCSs combine evolutionary algorithms with supervised learning to optimize fuzzy classification rules, offering enhanced interpretability and robustness. Despite these advantages, research on improving decision-making mechanisms (i.e., class inference schemes) in LFCSs remains limited. Most LFCSs use voting-based or single-winner-based inference schemes. These schemes rely on classification performance on training data and may not perform well on unseen data, risking overfitting. To address these limitations, this article introduces a novel class inference scheme for LFCSs based on the Dempster-Shafer Theory of Evidence (DS theory). The proposed scheme handles uncertainty well. By using the DS theory, the scheme calculates belief masses (i.e., measures of belief) for each specific class and the “I don’t know” state from each fuzzy rule and infers a class from these belief masses. Unlike the conventional schemes, the proposed scheme also considers the “I don’t know” state that reflects uncertainty, thereby improving the transparency and reliability of LFCSs. Applied to a variant of LFCS (i.e., Fuzzy-UCS), the proposed scheme demonstrates statistically significant improvements in terms of test macro F1 scores across 30 real-world datasets compared to conventional voting-based and single-winner-based fuzzy inference schemes. It forms smoother decision boundaries, provides reliable confidence measures, and enhances the robustness and generalizability of LFCSs in real-world applications. Our implementation is available at <https://github.com/YNU-NakataLab/jUCS>. An extended abstract related to this work is available at <https://doi.org/10.36227/techrxiv.174900814.43483543/v1> [Shiraishi et al. 2025].

CCS Concepts: • **Computing methodologies** → **Rule learning; Vagueness and fuzzy logic; Reasoning about belief and knowledge**; *Genetic algorithms; Supervised learning by classification.*

Additional Key Words and Phrases: Learning Fuzzy-Classifier Systems, Evolutionary Machine Learning, Dempster-Shafer Theory, Class Inference, Fuzzy-UCS.

## ACM Reference Format:

Hiroki Shiraishi, Hisao Ishibuchi, and Masaya Nakata. 2025. A Class Inference Scheme With Dempster-Shafer Theory for Learning Fuzzy-Classifier Systems. *ACM Trans. Evol. Learn.* 1, 1, Article 1 (February 2025), 47 pages. <https://doi.org/10.1145/3717613>

\*Corresponding authors.

Authors’ addresses: **Hiroki Shiraishi**, Faculty of Engineering, Yokohama National University, Yokohama 240-8501, Japan, [shiraishi-hiroki-yw@ynu.jp](mailto:shiraishi-hiroki-yw@ynu.jp); **Hisao Ishibuchi**, Department of Computer Science and Engineering, Southern University of Science and Technology, Shenzhen 518055, China, [hisao@sustech.edu.cn](mailto:hisao@sustech.edu.cn); **Masaya Nakata**, Faculty of Engineering, Yokohama National University, Yokohama 240-8501, Japan, [nakata-masaya-tb@ynu.ac.jp](mailto:nakata-masaya-tb@ynu.ac.jp).

Permission to make digital or hard copies of all or part of this work for personal or classroom use is granted without fee provided that copies are not made or distributed for profit or commercial advantage and that copies bear this notice and the full citation on the first page. Copyrights for components of this work owned by others than the author(s) must be honored. Abstracting with credit is permitted. To copy otherwise, or republish, to post on servers or to redistribute to lists, requires prior specific permission and/or a fee. Request permissions from [permissions@acm.org](mailto:permissions@acm.org).

© 2025 Copyright held by the owner/author(s). Publication rights licensed to ACM.

2688-3007/2025/2-ART1 \$15.00  
<https://doi.org/10.1145/3717613>

## 1 INTRODUCTION

The decision-making process is the foundation of machine learning models and plays a crucial role in their effectiveness and efficiency [Breiman 2001]. Accurate decision-making ensures that a model can generalize from training data and correctly classify new data points. This is especially important in rule-based systems where the selection and application of rules directly impact the accuracy and reliability of predictions [Wilson 1995].

*Learning Classifier Systems* (LCSs) [Holland 1986] are a prominent evolutionary machine learning paradigm that combines evolutionary algorithms with supervised learning to optimize a set of rules for classification tasks. An LCS can construct adaptive and interpretable rules (i.e., local models) that learn from their environment and adapt over time. LCSs have been applied in various fields, such as data mining [Zhang et al. 2021], automatic design of ensemble modeling [Preen et al. 2021], health informatics [Yazdani 2020], and bioinformatics [Woodward et al. 2024], demonstrating their versatility and effectiveness. However, LCSs typically utilize crisp rules, which, although effective, may lack the interpretability and robustness necessary to handle real-world data characterized by uncertainty and noise [Shiraishi et al. 2023]. To address these limitations, we focus on *Learning Fuzzy-Classifier Systems* (LFCs) [Valenzuela-Rendón 1991], an extension of LCS that optimizes fuzzy rules instead of crisp ones. Fuzzy rules offer several advantages over crisp rules. Firstly, fuzzy rules use linguistic terms, such as *small*, *medium*, and *large*, to represent the antecedents of the rules, providing higher interpretability compared to crisp rules [Fernandez et al. 2019; Ishibuchi et al. 2004]. In this article, we use the term *interpretability* to refer to the ease with which humans can understand and intuitively grasp the meaning of fuzzy rules. Zadeh [1975] suggested that linguistic labels used in fuzzy rules are often more intuitive for humans to comprehend compared to precise numerical ranges (i.e., quantitative terms) used in crisp rules. This interpretability is crucial in fields where transparency is essential, such as healthcare and finance [Adadi and Berrada 2018]. Secondly, fuzzy rules exhibit greater robustness when dealing with uncertainty and noise in the data [Shoehle et al. 2011]. This robustness is vital for real-world applications where data is often incomplete and imprecise.

Various improvements have been made to LFCs to date. For example, Shiraishi et al. [2023] proposed a mechanism that evolutionarily optimizes the shapes of membership functions for each rule according to the problem being solved. Additionally, Nojima et al. [2023] introduced a reject option to enhance LFC reliability by discarding low-confidence inference results. Recently, several LFCs have been proposed to address multi-label classification problems [Omozaki et al. 2020, 2022], significantly expanding the applicability of LFCs. However, research on improving the decision-making mechanism, i.e., class inference schemes, is still limited. Even with optimal rules, an inappropriate class inference scheme can lead to incorrect outputs. Conversely, an appropriate scheme can produce correct results even without optimal rules. Thus, focusing on the decision-making mechanism is important for enhancing LFC performance.

In LFCs, there are two primary schemes for class inference: a *voting-based inference* [Bardossy and Duckstein 1995] and a *single-winner-based inference* [Ishibuchi et al. 1999]. The voting-based inference is an ensemble-based approach that makes decisions based on the consensus of multiple rules, potentially enhancing robustness and accuracy. In contrast, the single-winner-based inference relies solely on the rule that performs the best on training data, making it straightforward. To the best of our knowledge, most LFCs (e.g., [Li and Zhang 2024; Nojima et al. 2015; Orriols-Puig and Casillas 2011; Shoehle et al. 2011; Tadokoro et al. 2021]) employ either the voting-based inference or single-winner-based inference. However, both schemes infer a class based on the quality of rules, as measured by a fitness function that reflects classification accuracy on training data. While these schemes work well for training data, they may not necessarily translate to high performance on

unseen data. There is a risk that rules optimized for training data may overfit, capturing noise and specific patterns that do not generalize well to new data points.

To mitigate these issues, this article introduces a novel class inference scheme for LFCSs based on the *Dempster-Shafer Theory of Evidence* (DS theory) [Dempster 1967; Shafer 1976], which is a robust framework for reasoning and decision making under uncertainty and conflicting information [Yager and Liu 2008]. The DS theory assigns a measure of belief, known as *belief mass*, to information from various independent knowledge sources and combines them using *Dempster's rule of combination* [Shafer 1976]. The DS theory can be a good candidate for increasing the robustness and generalizability of LFCS, especially since it deals with uncertainty and is adept at aggregating multiple lines of evidence.

Our goal is to integrate the DS theory into the LFCS decision-making process to improve the system's ability to make reliable and accurate predictions for unseen data points. Specifically, in the proposed class inference scheme, when a new data point is presented, belief masses are calculated from the membership degree and weight vector of each fuzzy rule. The inference result is a consensus derived from combining these belief masses using Dempster's rule of combination. Unlike the conventional voting- and single-winner-based schemes, which focus solely on which specific class each rule supports, our proposed scheme also considers "floating votes", i.e., "I don't know" belief masses indicating uncertainty. This feature enhances the transparency and reliability of the LFCS inference results. In this article, the proposed class inference scheme is applied to the *Supervised Fuzzy-Classifer System* (Fuzzy-UCS) [Orriols-Puig et al. 2009], an LFCS designed for single-label classification problems.

The main contributions of this article are as follows:

- (1) To the best of our knowledge, this article is the first to incorporate the DS theory into LFCSs.
- (2) Our experimental results demonstrate that Fuzzy-UCS with the proposed class inference scheme significantly improves classification performance for real-world problems characterized by uncertainty and incomplete information. This improvement is notable when compared to two variants of Fuzzy-UCS that use the conventional voting- and single-winner-based class inference schemes.
- (3) The proposed class inference scheme forms smoother decision boundaries compared to conventional class inference schemes. This feature helps to achieve more accurate classification results in Fuzzy-UCS.
- (4) The proposed class inference scheme provides belief masses indicating the reliability of the classification result. For instance, if a new data point is presented in a region with sparse training data points, the inference scheme assigns a larger "I don't know" belief mass, reflecting lower confidence in the inference.

The structure of this article is as follows: Section 2 reviews relevant literature. Sections 3 and 4 provide overviews of Fuzzy-UCS and the DS theory, respectively. Section 5 details the proposed class inference scheme for LFCSs. Section 6 conducts comparative experiments using 30 real-world datasets for classification tasks. The experimental results are then evaluated and discussed. Section 7 provides analytical results to investigate the characteristics of each class inference scheme. Finally, Section 8 concludes this article.

## 2 RELATED WORK

### 2.1 Class Inference Schemes in LFCSs

In LFCSs, two predominant class inference schemes have been established [Ishibuchi et al. 2004; Orriols-Puig et al. 2009]. The first, a *voting-based inference* [Bardossy and Duckstein 1995], involves a decision-making process that relies on the aggregated product of membership degrees and fitness

values from multiple fuzzy rules. The second, a *single-winner-based inference* [Ishibuchi et al. 1999], designates the class of the single fuzzy rule with the largest product of a membership degree and a fitness value as the output. These schemes have found contemporary applications in modern LFCs, such as [Omozaki et al. 2022] and [Shiraishi et al. 2023]. Notably, the voting-based inference has been adapted for nonfuzzy-classifier systems and is now a standard class inference scheme in leading LCSs, such as XCS [Wilson 1995], UCS [Bernadó-Mansilla and Garrell-Guiu 2003], ExSTraCS [Urbanowicz and Moore 2015], and ASCS [Liu et al. 2020].

## 2.2 Dempster-Shafer Theory in Rule-Based Systems

The integration of the DS theory into rule-based systems has been explored across various domains. While this article focuses on its application within LFCs, the DS theory has also been employed in expert systems to enhance decision-making under uncertainty.

For example, Guth [1988] applied the DS theory to analyze uncertainty propagation in rule-based expert systems, demonstrating its effectiveness in handling both probabilistic rule assignments and uncommitted belief in Boolean logic frameworks. Beynon et al. [2001] developed an expert system using the DS theory combined with the Analytic Hierarchy Process for multi-criteria decision-making, showcasing its application in real estate property evaluation. Similarly, Hutasuht et al. [2018] developed an expert system using the DS theory to detect stroke, demonstrating its effectiveness in medical diagnostics by providing optimal diagnoses based on patient symptoms.

These examples highlight how the DS theory can improve decision-making in various fields. This wide applicability provides a solid basis for using the DS theory in LFCs, as we proposed in this article.

## 2.3 Dempster-Shafer Theory in Machine Learning

The integration of the DS theory into machine learning was first exemplified by Denœux [1995], who enhanced the traditional k-nearest neighbors (kNN) method by combining pieces of evidence from each data point's neighborhood. Following this pioneering work, numerous machine learning techniques, such as decision trees [Quinlan 1993], support vector machines [Boser et al. 1992], fuzzy c-means [Bezdek 2013], Naïve Bayes [John and Langley 1995], and LCS, have leveraged the strengths of the DS theory in managing uncertainty and merging evidence from diverse sources [Ferjani et al. 2024; Li et al. 2019; Masson and Denœux 2008; Mulyani et al. 2016; Zhou et al. 2015].

A notable recent advance is the introduction of the DS theory into deep learning by Sensoy et al. [2018], which quantifies the uncertainty in classification results. Their methodology differs from traditional neural networks in that it produces parameters of a Dirichlet distribution, based on the DS theory, to model both predictions and uncertainties in classification. These parameters facilitate the calculation of predictive probabilities for each class and uncertainty.

The DS theory has been employed not only in individual machine learning models but also for integrating outputs from multiple models [Belmahdi et al. 2023; Gudiyangada Nachappa et al. 2020; Rahmati and Melesse 2016]. For instance, Belmahdi et al. [2023] demonstrated that combining the inference results of three classifiers (artificial neural network, support vector machine, and random forest [Breiman 2001]) using the DS theory can lead to improved classification results compared to those relying on a single classifier.

Although the DS theory has been successfully applied in machine learning, its use in LFCs has not been explored.

## 3 FUZZY-UCS

Fuzzy-UCS [Orriols-Puig et al. 2009] is a Michigan-style LFCS that integrates supervised learning with a steady-state genetic algorithm (GA) [Goldberg 2002] to evolve fuzzy rules online. Essentially,

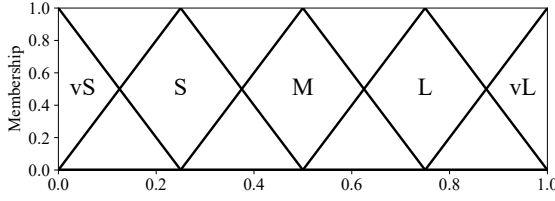


Fig. 1. An example of homogeneous linguistic discretization of the domain interval  $[0, 1]$ . The meaning of each term is as follows: vS: *very small*, S: *small*, M: *medium*, L: *large*, vL: *very large*.

Fuzzy-UCS can be viewed as a “fuzzified” adaptation of UCS [Bernadó-Mansilla and Garrell-Guiu 2003]. This system alternates between two primary phases: the training (*exploration*) phase and the test (*exploitation*) phase. Within the training phase, Fuzzy-UCS searches for accurate and maximally general rules. Conversely, during the test phase, the system applies these acquired rules to infer a class for a new unlabeled data point. This section briefly explains Fuzzy-UCS for a  $d$ -dimensional  $n$ -class single-label classification problem with a class label set  $C = \{c_i\}_{i=1}^n$ . For detailed explanations, kindly refer to [Orriols-Puig et al. 2009].

### 3.1 Knowledge Representation

A  $d$ -dimensional fuzzy rule  $k$  is expressed by:

$$\text{IF } x_1 \text{ is } A_1^k \text{ and } \dots \text{ and } x_d \text{ is } A_d^k \text{ THEN } c^k \text{ WITH } w^k, \quad (1)$$

where  $A^k = (A_1^k, \dots, A_d^k)$  is a *rule-antecedent* vector,  $c^k \in C = \{c_1, \dots, c_n\}$  is a *rule-consequent* class, and  $w^k \in [0, 1]$  is a *rule-weight*. Each variable  $x_i$  is conditioned by a fuzzy set  $A_i$  for  $\forall i \in \{1, \dots, d\}$ . In this article, as the antecedent set, we use a triangular-shaped membership function with five linguistic terms in Fig. 1. The Fuzzy-UCS framework can optimize the shape of membership functions by using the GA to search for the optimal combination of linguistic labels for each rule.

The *membership degree*  $\mu_{A^k}(\mathbf{x}) \in [0, 1]$  of an input vector  $\mathbf{x} \in [0, 1]^d$  with the rule  $k$  in Eq. (1) is calculated by the product operator:

$$\mu_{A^k}(\mathbf{x}) = \prod_{i=1}^d \mu_{A_i^k}(x_i), \quad (2)$$

where  $\mu_{A_i^k} : [0, 1] \rightarrow [0, 1]$  is the membership function of the fuzzy set  $A_i^k$ . If the value of  $x_i$  is unknown, the system handles the missing value by specifying  $\mu_{A_i^k}(x_i) = 1$ .

Each rule  $k$  has six primary parameters: (i) a *fitness*  $F^k \in (-1, 1]$ , which reflects the classification accuracy of rule  $k^1$ ; (ii) a *weight vector*  $\mathbf{v}^k = (v_i^k)_{i=1}^n \in [0, 1]^n$ , indicating the confidence with which rule  $k$  predicts each class  $c_i$  for a matched input (the largest element of  $\mathbf{v}^k$  is used as  $w^k$  in Eq. (1)); (iii) a *correct matching vector*  $\mathbf{cm}^k = (cm_i^k)_{i=1}^n \in (\mathbb{R}_0^+)^n$ , where each element  $cm_i^k$  is the summation of the membership degree for training data points from class  $c_i$ ; (iv) an *experience*  $\exp^k \in \mathbb{R}_0^+$ , which computes the accumulated contribution of rule  $k$  in order to classify training data points; (v) a *numerosity*  $\text{num}^k \in \mathbb{N}_0$ , which indicates the number of rules that have been subsumed (i.e.,

<sup>1</sup>In LCSs (such as UCS and ExSTraCS), fitness values range between  $(0, 1]$ . In contrast, in LFCSs like Fuzzy-UCS, fitness values range between  $(-1, 1]$  due to the fitness calculation method introduced by [Ishibuchi and Yamamoto 2005], as described in Section 3.2.1. [Ishibuchi and Yamamoto 2005] demonstrated that employing fitness values within the  $(-1, 1]$  range enhances the test classification accuracy of an LFCS compared to the  $(0, 1]$  range. Consequently, Fuzzy-UCS also adopts fitness values within the  $(-1, 1]$  range in their original work [Orriols-Puig et al. 2009]. For further details, kindly refer to Appendix A.

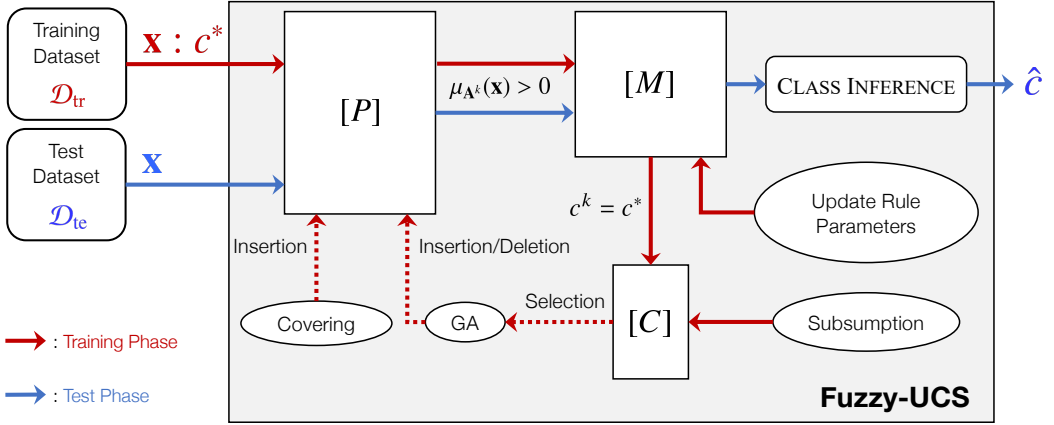


Fig. 2. Schematic illustration of Fuzzy-UCS. The run cycle depends on the type of run: training or test. Upon receiving each data point  $\mathbf{x}$ , operations indicated by solid arrows are always performed, while operations indicated by dashed arrows (i.e., covering and GA) are executed only when specific conditions are met (cf. Section 3.2.1).

the number of successful *subsumption* operations, detailed in Section 3.2.1); and (vi) a *time stamp*  $ts^k \in \mathbb{N}$ , which denotes the time-step of the last execution of a steady-state GA to create new rules, where rule  $k$  was considered as a candidate to be a parent. These parameters are continuously updated throughout the training process.

### 3.2 Algorithm

Fig. 2 schematically illustrates Fuzzy-UCS.

**3.2.1 Training Phase.** Algorithm 1 describes the whole procedure of Fuzzy-UCS during the training phase. At time  $t = 0$ , the *ruleset*  $[P]$  is initialized as an empty set (lines 1-2). Each training data point in a training dataset  $\mathcal{D}_{tr}$  is used for a pre-specified number of epochs (e.g., 10 epochs) in a random order, which is the termination criteria of the training phase.

All rules are stored in  $[P]$ . At time  $t$ , the system receives a data point  $\mathbf{x}$  from  $\mathcal{D}_{tr}$  (line 4). Subsequently, a *match set*  $[M] = \{k \in [P] \mid \mu_{A^k}(\mathbf{x}) > 0\}$  is constructed (line 5). Let  $c^*$  be the class of this data point (line 6). After  $[M]$  is formed, the system forms a *correct set*  $[C] = \{k \in [M] \mid c^k = c^*\}$  (line 7). If  $\sum_{k \in [C]} \mu_{A^k}(\mathbf{x}) < 1$  is satisfied<sup>2</sup>, the *covering* operator generates a new rule  $k_{cov}$  such that  $\mu_{A^{k_{cov}}}(\mathbf{x}) = 1$ ,  $c^{k_{cov}} = c^*$ , and  $v_i^{k_{cov}} = 1$  if  $c_i = c^*$  else 0 for  $\forall i \in \{1, \dots, n\}$  (lines 8-10).

After  $[C]$  is formed, the parameters of all rules in  $[M]$  are updated (line 11). First, the experience of each rule  $k$  in  $[M]$  is updated according to the current membership degree using<sup>3</sup>:

$$\exp_{t+1}^k = \exp_t^k + \mu_{A^k}(\mathbf{x}). \quad (3)$$

<sup>2</sup>If no rules match a data point (i.e.,  $[M] = \emptyset$ ), then  $[C] = \emptyset$  and  $\sum_{k \in [C]} \mu_{A^k}(\mathbf{x}) = 0$ , satisfying the condition  $\sum_{k \in [C]} \mu_{A^k}(\mathbf{x}) < 1$ . This triggers the covering operator to generate a new rule, ensuring the data point is covered.

<sup>3</sup>Unlike the membership degree-based update method in Fuzzy-UCS, in LCSs (such as UCS and ExSTraCS), the experience is updated incrementally using  $\exp_{t+1}^k = \exp_t^k + 1$ , uniformly increasing the experience of all matched rules. Our comparative experiments showed that Fuzzy-UCS with membership degree-based updates consistently achieved higher accuracy than the method that incrementally increased the experience by one. For further details, kindly refer to Appendix B.

**Algorithm 1** Fuzzy-UCS training phase, adapted from [Orriols-Puig et al. 2009] ▶ Section 3.2.1**Input:** the training dataset  $\mathcal{D}_{tr}$ ;**Output:** the ruleset  $[P]$ ;

```

1: Initialize time  $t$  as  $t \leftarrow 0$ ;
2: Initialize ruleset  $[P]$  as  $[P] \leftarrow \emptyset$ ;
3: while termination criteria are not met do
4:   Observe a data point  $\mathbf{x} \in \mathcal{D}_{tr}$ ;
5:   Create match set  $[M] := \{k \in [P] \mid \mu_{A^k}(\mathbf{x}) > 0\}$ ;
6:   Observe correct class  $c^* \in C$  associated with  $\mathbf{x}$ ;
7:   Create correct set  $[C] := \{k \in [M] \mid c^k = c^*\}$ ;
8:   if  $\sum_{k \in [C]} \mu_{A^k}(\mathbf{x}) < 1$  then
9:     Execute covering operator to generate a new rule  $k_{cov}$ ;
10:  end if
11:  Update  $\exp^k$ ,  $\mathbf{cm}^k$ ,  $\mathbf{v}^k$ , and  $F^k$  for  $\forall k \in [M]$  as in Eqs. (3)-(6);
12:  Do correct set subsumption if necessary;
13:  if  $t - \sum_{k \in [C]} \text{num}^k \cdot \text{ts}^k / \sum_{k \in [C]} \text{num}^k > \theta_{GA}$  then
14:    Update  $\text{ts}^k$  for  $\forall k \in [C]$  as  $\text{ts}^k \leftarrow t$ ;
15:    Run GA on  $[C]$ ;
16:    Do GA subsumption if necessary;
17:  end if
18:  Update  $t$  as  $t \leftarrow t + 1$ ;
19: end while

```

Next, the fitness is updated. To accomplish this, the system first updates the correct matching vector for  $\forall c_i \in C$  as:

$$\mathbf{cm}_{i_{t+1}}^k = \begin{cases} \mathbf{cm}_{i_t}^k + \mu_{A^k}(\mathbf{x}) & \text{if } c_i = c^*, \\ \mathbf{cm}_{i_t}^k & \text{otherwise.} \end{cases} \quad (4)$$

Then, the system updates the weight for  $\forall c_i \in C$  using:

$$v_{i_{t+1}}^k = \frac{\mathbf{cm}_{i_{t+1}}^k}{\exp_{t+1}^k}, \quad (5)$$

where  $v_i^k$  indicates the soundness of which rule  $k$  predicts class  $c_i$  for a matched input. Note that the value of  $\sum_{i=1}^n v_i^k$  is always 1. After that, the system updates the fitness using:

$$F_{t+1}^k = v_{\max_{t+1}}^k - \sum_{i \mid i \neq \max} v_{i_{t+1}}^k, \quad (6)$$

where the system subtracts the values of the other weights from the weight with maximum value  $v_{\max}^k$  [Ishibuchi and Yamamoto 2005]. Finally, the highest weight  $v_{\max}^k$  in the weight vector  $\mathbf{v}^k$  and its corresponding class label  $c_{\max}$  are designated as the rule-weight  $w^k$  and the rule-consequent class  $c^k$  in Eq. (1), respectively.

After the rule update, a steady-state GA is applied to  $[C]$  (lines 13-17). Michigan-style LFCSS (e.g., Fuzzy-XCS [Casillas et al. 2007] and Fuzzy-UCS) are designed to call the GA after an interval of a given number of inputs controlled by the hyperparameter  $\theta_{GA}$  [Nakata and Browne 2021]. More specifically, the GA is executed when  $t - \frac{\sum_{k \in [C]} \text{num}^k \cdot \text{ts}^k}{\sum_{k \in [C]} \text{num}^k} > \theta_{GA}$  is satisfied. In this case, the two parent rules from  $[C]$  excluding any rules with negative fitness are selected through tournament

**Algorithm 2** Fuzzy-UCS test phase, adapted from [Orriols-Puig et al. 2009] ▷ Section 3.2.2**Input:** a data point  $\mathbf{x}$  from the test dataset  $\mathcal{D}_{te}$ , the ruleset  $[P]$ ;**Output:** the inferred class label  $\hat{c}$  of  $\mathbf{x}$ ;

- 1: Create match set  $[M] := \{k \in [P] \mid \mu_{A^k}(\mathbf{x}) > 0\}$ ;
- 2: Filter  $[M]$  as  $[M] \leftarrow \{k \in [M] \mid \exp^k > \theta_{exploit}\}$ ;
- 3: **if**  $[M] \neq \emptyset$  **then**
- 4:      $\hat{c} \leftarrow \text{CLASSINFERENCE}([M], \mathbf{x})$ ;
- 5: **else**
- 6:      $\hat{c} \leftarrow$  a randomly chosen class;
- 7: **end if**

selection, with the tournament size determined by the hyperparameter  $\tau$ . This mechanism enables the GA to guide the system in systematically eliminating inaccurate rules, thereby enhancing the performance of the system. The two parent rules are replicated as two child rules, and then crossover and mutation are applied to the two child rules with probabilities  $\chi$  and  $p_{mut}$ , respectively. The two child rules are inserted into  $[P]$  and two rules are deleted if the number of rules in  $[P]$ ,  $\sum_{k \in [P]} \text{num}^k$ , exceeds the ruleset size  $N$ .

The *subsumption* operator [Wilson 1998] can be employed to prevent inserting over-specific rules into the ruleset [Liu et al. 2020]. Subsumption is triggered after  $[C]$  is formed or after GA is executed, and is referred to as *Correct Set Subsumption* (line 12) and *GA Subsumption* (line 16), respectively. Specifically, for the two rules  $k_{sub}$  and  $k_{tos}$ , if (i)  $k_{sub}$  is more general than  $k_{tos}$  (i.e.,  $k_{sub}$  has at least the same linguistic terms per variable as  $k_{tos}$ ); (ii)  $k_{sub}$  is accurate (i.e.,  $F^{k_{sub}}$  is greater than the hyperparameter  $F_0$ ); and (iii)  $k_{sub}$  is sufficiently experienced (i.e.,  $\exp^{k_{sub}}$  is greater than the hyperparameter  $\theta_{sub}$ ), then  $k_{tos}$  is removed from  $[P]$ , and the numerosity of  $k_{sub}$  is updated using  $\text{num}_{t+1}^{k_{sub}} = \text{num}_t^{k_{sub}} + \text{num}_t^{k_{tos}}$  to record the number of subsumed rules.

**3.2.2 Test Phase.** Algorithm 2 describes the whole procedure of Fuzzy-UCS during the test phase.

Given a data point  $\mathbf{x}$  from a test dataset  $\mathcal{D}_{te}$ , the system's output  $\hat{c}$  is determined through class inference using multiple rules in the match set  $[M]$ . This subsection outlines two inference schemes (cf. Section 2.1 and line 4). It is important to note that only rules with sufficient experience (i.e.,  $\exp^k$  is greater than the hyperparameter  $\theta_{exploit}$ ) are considered for inference (line 2).

**Voting-based inference.** The system's output  $\hat{c}$  is determined using:

$$\hat{c} = \arg \max_{c \in C} \sum_{k \in [M_c]} \mu_{A^k}(\mathbf{x}) \cdot F^k \cdot \text{num}^k, \quad (7)$$

where  $[M_c]$  represents the subset of rules in  $[M]$  with a consequent class of  $c$ . Here,  $\mu_{A^k}(\mathbf{x}) \cdot F^k \cdot \text{num}^k$  represents the votes a rule  $k$  has. The class with the highest number of votes is then the output  $\hat{c}$ .

**Single-winner-based inference.** The system's output  $\hat{c}$  is determined using:

$$\hat{c} = c^{k^*}, \quad \text{where } k^* = \arg \max_{k \in [M]} \left( \mu_{A^k}(\mathbf{x}) \cdot F^k \right). \quad (8)$$

Here,  $k^*$  is the single-winner rule that maximizes  $\mu_{A^k}(\mathbf{x}) \cdot F^k$  among all the rules in  $[M]$ . The consequent class  $c^{k^*}$  of this rule  $k^*$  is then the output  $\hat{c}$ .

It is worth noting that, for both inference schemes, the system's output  $\hat{c}$  is determined randomly if there are no rules that allow participation in inference (i.e.,  $[M] = \emptyset$ , line 6). In case of a tie, such as when the total votes for  $c_1$  and  $c_2$  are equal in the voting-based inference,  $\hat{c}$  is randomly selected from the tied classes (i.e.,  $c_1$  and  $c_2$ ).

## 4 DEMPSTER-SHAFFER THEORY OF EVIDENCE

The *Dempster-Shafer Theory of Evidence* (DS theory) was introduced by Shafer [1976] as a reformation of Dempster's earlier work [1967]. It offers a robust framework for reasoning with uncertainty. This section outlines the fundamental concepts of the DS theory that are important for understanding the proposed class inference scheme.

### 4.1 Frame of Discernment

The *frame of discernment*, denoted as  $\Theta = \{\theta_1, \theta_2, \dots, \theta_n\}$ , represents a finite set of distinct, mutually exclusive hypotheses  $\theta_i$ . Each subset of  $\Theta$  can be viewed as a composite hypothesis, leading to a total of  $|2^\Theta|$  possible hypotheses, where  $2^\Theta$  denotes the power set of  $\Theta$ . For instance, if  $\Theta = \{\theta_1, \theta_2, \theta_3\}$ , then  $2^\Theta$  encompasses the following eight subsets:  $\{\emptyset, \{\theta_1\}, \{\theta_2\}, \{\theta_3\}, \{\theta_1, \theta_2\}, \{\theta_1, \theta_3\}, \{\theta_2, \theta_3\}, \Theta\}$ .

In the context of an  $n$ -class classification problem with a class label set  $C = \{c_i\}_{i=1}^n$ , a subset such as  $\{\theta_1\}$  represents the hypothesis "the class of a given data point is  $c_1$ ", implying a specific class determination. A subset like  $\{\theta_1, \theta_2\}$  suggests "the class of the given data point is either  $c_1$  or  $c_2$ ", denoting partial ignorance or a meta-class.  $\Theta$  as a whole implies complete uncertainty about the class (i.e., any class in  $C$ ), representing a complete ignorance, uncertainty, or an "I don't know" state [Sensoy et al. 2018]. Conversely, the empty set  $\emptyset$  denotes a hypothesis that is considered impossible or improbable (i.e., no class in  $C$ ).

### 4.2 Belief Mass Function

Within the DS theory framework, the concept of a *belief mass function* is important. This function, denoted as  $m : 2^\Theta \rightarrow [0, 1]$ , assigns a degree of belief, referred to as *belief mass*, to each hypothesis within the frame of discernment. The belief mass function adheres to specific criteria outlined in the following equations:

$$m(A) \geq 0, \quad \forall A \in 2^\Theta, \quad (9)$$

$$m(\emptyset) = 0, \quad (10)$$

$$\sum_{A \in 2^\Theta} m(A) = 1. \quad (11)$$

The belief mass  $m(A)$  is interpreted as the specific degree of belief committed solely to the hypothesis  $A$  and not to any of its subsets. In this context, subsets  $A$  of  $\Theta$  for which  $m(A) > 0$  are termed *focal elements* of  $m$ . The collection of all such focal elements constitutes the *core* of  $m$  [ga Liu et al. 2013]. The condition  $m(\emptyset) = 0$  is a fundamental requirement in the DS theory. Shafer [Shafer 1976] introduced it as the normality condition. It ensures that no belief is assigned to the empty set (i.e., to an impossible hypothesis).

### 4.3 Combination of Belief Masses

The DS theory employs a specific operator known as *Dempster's rule of combination* [Shafer 1976] for fusing information from distinct, independent sources of knowledge. This process involves the following steps.

Initially, the *conjunctive sum* of two belief mass functions  $m_1$  and  $m_2$ , corresponding to every hypothesis  $\forall A \in 2^\Theta$ , is computed. This is achieved through the following formula called *conjunctive rule of combination* [Smets 1990]:

$$(m_1 \cap m_2)(A) \triangleq \sum_{B \cap C = A} m_1(B) \cdot m_2(C). \quad (12)$$

Subsequently, using Dempster's rule of combination, the functions  $m_1$  and  $m_2$  are combined as follows:

$$(m_1 \oplus m_2)(A) \triangleq \frac{1}{1 - \mathcal{K}_{12}} (m_1 \cap m_2)(A), \quad (13)$$

where  $\mathcal{K}_{12} \triangleq (m_1 \cap m_2)(\emptyset)$  quantifies the *conflict* between  $m_1$  and  $m_2$ . The term  $\mathcal{K}_{12}$  is referred to as the *mass of conflict* [Kessentini et al. 2015]. A higher value of  $\mathcal{K}_{12}$ , signifies greater inconsistency between the two sets of information. The normalization factor  $\frac{1}{1 - \mathcal{K}_{12}}$  reallocates the belief mass that is lost due to contradictions, distributing it among the non-contradictory elements (i.e., focal elements). This adjustment ensures that the conditions in Eqs. (10) and (11) remain valid.

It is worth noting that both the conjunctive rule of combination,  $\cap$ , and Dempster's rule of combination,  $\oplus$ , exhibit properties of commutativity and associativity [Lefevre et al. 2002; Smets 1990]. This allows for flexibility in the order and grouping of information combinations.

#### 4.4 Pignistic Transform

The *transferable belief model* (TBM) [Smets and Kennes 1994] is a framework for reasoning under uncertainty that distinguishes between belief representation and decision-making. Within this framework, the *pignistic transform* [Smets and Kennes 1994] plays a crucial role in bridging these two aspects. The term "pignistic" comes from the Latin word "pignus," meaning a bet, emphasizing its role in decision-making processes [Smets 2000].

The pignistic transform is a process that converts the belief mass function  $m$  into a form of probability, called *pignistic probability*. This transformation is necessary because while belief functions are excellent for representing uncertainty and partial knowledge, they are not directly suitable for decision-making. The resulting pignistic probability provides a basis for making decisions using the expected utility theory [Smets 2005]. The pignistic probability for any hypothesis within the frame of discernment  $\forall \theta \in \Theta$  is calculated as follows:

$$\text{BetP}(\theta) \triangleq \sum_{\theta \in A \subseteq \Theta} \frac{m(A)}{|A|}, \quad (14)$$

where  $|A|$  represents the cardinality (i.e., number of elements) of the subset  $A$ . The pignistic probability is computed by distributing the belief mass  $m(A)$  of each subset  $A$  of  $\Theta$  equally among the elements in  $A$ . This distribution process is based on the concept of fairness, especially in the context of ambiguity or partial ignorance [Kessentini et al. 2015].

Pignistic probabilities are particularly valuable in decision-making under uncertainty or when dealing with incomplete information. By transforming belief masses into a more interpretable and actionable form, the pignistic transform helps to derive clear and rational decisions from complex and uncertain data [ga Liu et al. 2013].

## 5 THE PROPOSED CLASS INFERENCE SCHEME

### 5.1 Overview

This section proposes a novel class inference scheme for the test phase of LFCSs. The proposed scheme effectively incorporates the DS theory into the LFCS framework. It achieves this by quantifying and combining multiple pieces of information, namely the membership degrees of rules and their associated weight vectors. These elements are derived from various independent knowledge sources, namely fuzzy rules acquired by an LFCS, and are treated as belief masses within the DS theory framework. This approach aims to enhance the LFCS's ability to perform more accurate and reliable class inference, especially in situations characterized by complexity and uncertainty.

## 5.2 Algorithm

Fig. 3 schematically illustrates the algorithm. Algorithm 3 describes the whole procedure of the proposed class inference scheme. The algorithm is designed for an  $n$ -class single-label classification problem with a class label set  $C = \{c_i\}_{i=1}^n$ . In the algorithm,  $\Theta = \{\theta_i\}_{i=1}^n$  is the frame of discernment. This frame consists of a finite set of hypotheses  $\theta_i$  each of which corresponds to a specific class label  $c_i$ . The proposed inference scheme follows these steps:

- (1) **Construction of Belief Mass Function.** Formulate a belief mass function for each fuzzy rule in the match set  $[M]$ . This function is based on the rule's membership degree  $\mu_{A^k}(\mathbf{x})$  and a weight vector  $\mathbf{v}^k$  (detailed in Section 5.2.1).
- (2) **Combination of Belief Masses.** Integrate the belief masses of all fuzzy rules in  $[M]$  to form a combined belief mass, denoted as  $m_{[M]}$  (detailed in Section 5.2.2).
- (3) **Pignistic Transform and Decision-Making.** Apply the pignistic transform to  $m_{[M]}$  and determine the class with the highest pignistic probability. This class is then selected as the inference result  $\hat{c}$  (detailed in Section 5.2.3).

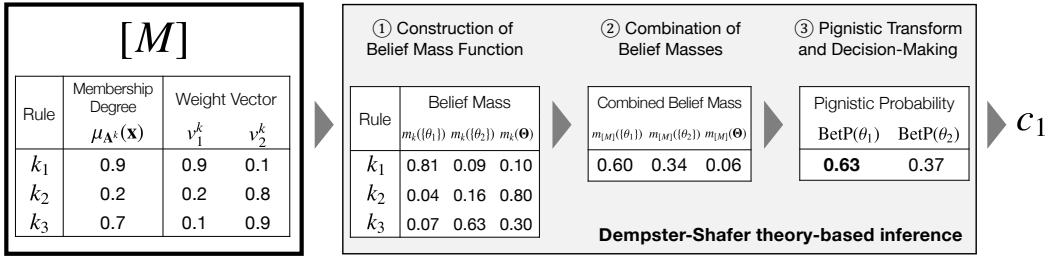


Fig. 3. An example of how the proposed class inference scheme works for an input data point  $\mathbf{x}$  on a binary classification problem with a class label set  $C = \{c_1, c_2\}$ .

---

### Algorithm 3 Dempster-Shafer theory-based inference

▷ Section 5.2

- 1: **function** CLASSINFERENCE( $[M], \mathbf{x}$ ) ▷ cf. Alg. 2, line 4
  - 2:     Construct belief mass function  $m_k(A)$  for  $\forall k \in [M]$  as in Eq. (15);
  - 3:     Calculate the mass of conflict  $\mathcal{K}_{[M]}$  as in Eq. (16);
  - 4:     Calculate the combined belief mass  $m_{[M]}(A)$ :
  - 5:     **if**  $\mathcal{K}_{[M]} \neq 1$  **then**
  - 6:         Using Dempster's rule of combination as in Eq. (17);
  - 7:     **else**
  - 8:         Using Yager's rule as in Eq. (18);
  - 9:     **end if**
  - 10:     Construct pignistic probability BetP( $\theta$ ) for  $\forall \theta \in \Theta$  as in Eq. (14);
  - 11:     **return** the best hypothesis in  $\Theta$  as in Eq. (19);
  - 12: **end function**
-

5.2.1 *Construction of Belief Mass Function.* The belief mass function  $m_k(A)$  for a given rule  $k \in [M]$ , corresponding to every hypothesis  $\forall A \in 2^\Theta$ , is defined as follows (line 2):

$$m_k(A) = \begin{cases} \mu_{A^k}(\mathbf{x}) \cdot v_i^k & \text{if } A \in \{\{\theta_i\}\}_{i=1}^n, \\ 1 - \sum_{i=1}^n m_k(\{\theta_i\}) & \text{if } A = \Theta, \\ 0 & \text{otherwise.} \end{cases} \quad (15)$$

This definition assigns the belief mass to each hypothesis as follows:

- For any specific class hypothesis  $A \in \{\{\theta_i\}\}_{i=1}^n$  (a singleton set), the belief mass is the product of the membership degree  $\mu_{A^k}(\mathbf{x})$  and the class-specific weight  $v_i^k$ .
- For the hypothesis  $\Theta$ , which represents complete ignorance or uncertainty about the class, the belief mass is set to the remainder of the belief mass after accounting for all specific classes. This is computed as 1 minus the sum of belief masses for all specific class hypotheses.
- For any other hypotheses (combinations of classes or meta-classes), the belief mass is set to 0.

This approach ensures that the sum of belief masses across all hypotheses equals 1, as required by the DS theory (cf. Eq. (11)). By allocating the residual belief to the hypothesis of complete ignorance  $\Theta$ , the system maintains a balance between certainty (specific class hypotheses) and uncertainty (complete ignorance), reflecting a comprehensive view of the class distribution for the given input.

This approach is similar to methods used in machine learning techniques that apply the DS theory to single-label classification problems. Examples include [Sensoy et al. 2018] and [Belmahdi et al. 2023]. In these techniques, the core's maximum size is typically set to  $n + 1$ . This size accounts for  $n$  specific class hypotheses and one hypothesis representing complete ignorance.

5.2.2 *Combination of Belief Masses.* This process combines the belief mass functions of all fuzzy rules within  $[M]$  into a single belief mass function  $m_{[M]}$ . The goal of this step is to obtain the belief mass  $m_{[M]}(A)$  for every hypothesis  $\forall A \in 2^\Theta$ .

Initially, the mass of conflict  $\mathcal{K}_{[M]}$  among all rules in  $[M]$  is calculated using the conjunctive sum operator (line 3):

$$\mathcal{K}_{[M]} = \left( \bigcap_{k \in [M]} m_k \right) (\emptyset). \quad (16)$$

If  $\mathcal{K}_{[M]} < 1$ , which means that the belief masses of the rules in  $[M]$  do not entirely contradict one another, the combined belief mass  $m_{[M]}(A)$  is calculated using Dempster's rule of combination (line 6):

$$m_{[M]}(A) = \left( \bigoplus_{k \in [M]} m_k \right) (A) = \frac{1}{1 - \mathcal{K}_{[M]}} \left( \bigcap_{k \in [M]} m_k \right) (A). \quad (17)$$

Conversely, if  $\mathcal{K}_{[M]} = 1$ , which means the complete contradiction in the information from the rules in  $[M]$ , Dempster's rule of combination becomes inapplicable due to the issue of division by zero. In this case, *Yager's rule* [Yager 1987] is utilized to address this contradiction (line 8):

$$m_{[M]}(A) = \begin{cases} 1 & \text{if } A = \Theta, \\ 0 & \text{otherwise.} \end{cases} \quad (18)$$

Eq. (18) handles a complete contradiction between independent knowledge sources as a state of "complete lack of knowledge that resolves the contradiction." [Yager 1987] It resolves this contradiction by reassigning the mass of conflict  $\mathcal{K}_{[M]} = 1$  to the belief mass of complete ignorance  $\Theta$ . This

approach manages contradictions by acknowledging them as a lack of sufficient information to resolve the conflict.

**5.2.3 Pignistic Transform and Decision-Making.** To make the final decision, the proposed class inference scheme utilizes a pignistic transform on the combined belief mass function  $m_{[M]}$ . This transformation yields the pignistic probability  $\text{BetP}(\theta)$  for each hypothesis  $\theta$  within the frame of discernment  $\Theta$ , as formulated in Eq. (14) (line 10).

The decision-making process involves selecting the class  $c_i$  associated with the hypothesis  $\{\theta_i\}$  that has the highest pignistic probability. This is represented as follows (line 11):

$$\hat{c} = \arg \max_{\theta \in \Theta} \text{BetP}(\theta), \quad (19)$$

where  $\hat{c}$  denotes the inferred class label, which is determined based on the maximum pignistic probability among all considered hypotheses (i.e., all classes). This approach ensures that class inference is based on a comprehensive assessment of the evidence gathered from the fuzzy rules in  $[M]$ .

When there are ties with multiple hypotheses having the same highest pignistic probability, the system randomly chooses the output  $\hat{c}$  from the tied classes, similar to the conventional class inference schemes (cf. Section 3.2.2). Such situations typically arise when  $m_{[M]}(\Theta) = 1$  according to Yager's rule. In these cases, the pignistic probability for each hypothesis  $\theta_i$  is equally distributed according to Eq. (14). This approach ensures that the system can still generate a randomly selected output in cases where information is either completely uncertain or contradictory.

## 6 EXPERIMENTS

This section utilizes 30 real-world datasets in Table 1 from the *UCI Machine Learning Repository* [Dua and Graff 2017] and *Kaggle Dataset* collection. These datasets are selected due to their inherent challenges in data classification, such as the presence of missing values and class imbalance issues [Thumpati and Zhang 2023].

Our objective is to evaluate the impact of different class inference schemes on the classification accuracy of LFCs. To accomplish this, we compare the performance of three Fuzzy-UCS\* variants. Here, \* is the abbreviation of the inference scheme used in Fuzzy-UCS. The abbreviations are defined as follows: (i) VOTE, for the voting-based inference scheme; (ii) SWIN, for the single-winner-based inference scheme; and (iii) DS, for the proposed DS theory-based inference scheme. It is important to note that all three Fuzzy-UCS\* variants utilize the same ruleset,  $[P]$ , produced during the training phase. This ensures a fair comparison across the different inference schemes. Additionally, to provide a comprehensive evaluation of the proposed scheme, we include a well-known LCS, the UCS nonfuzzy-classifier system [Bernadó-Mansilla and Garrell-Guiu 2003], in our comparison.

### 6.1 Experimental Setup

For all of the considered problems, the hyperparameters for UCS and Fuzzy-UCS\* are set to the values based on [Orriols-Puig et al. 2009; Tzima and Mitkas 2013; Urbanowicz and Moore 2015], as shown in Table 2. For more information on the hyperparameters, kindly refer to [Bernadó-Mansilla

<sup>4</sup><https://www.kaggle.com/datasets/erdemtaha/cancer-data> (June 12, 2025)

<sup>5</sup><https://www.kaggle.com/datasets/deepatharwani/car-acceptance-datasets> (June 12, 2025)

<sup>6</sup><https://www.kaggle.com/datasets/torikul140129/paddy-leaf-images-aman> (June 12, 2025)

<sup>7</sup><https://www.kaggle.com/datasets/yoshifumimiya/pharyngitis/data> (June 12, 2025)

<sup>8</sup><https://www.kaggle.com/datasets/micheldc55/predicting-response-based-on-engagement-kpis> (June 12, 2025)

<sup>9</sup><https://www.kaggle.com/datasets/devzohaib/smoker-condition> (June 12, 2025)

<sup>10</sup><https://www.kaggle.com/datasets/tejashvi14/travel-insurance-prediction-data> (June 12, 2025)

<sup>11</sup><https://www.kaggle.com/datasets/yasserh/titanic-dataset> (June 12, 2025)

Table 1. Properties of the 30 Real-World Datasets. The Columns Describe: the Identifier (ID.), the Name (Name), the Number of Instances (#INST.), the Total Number of Features (#FEA.), the Number of Classes (#CL.), the Percentage of Missing Attributes (%MIS.), the Percentage of Instances of the Majority Class (%MAJ.), the Percentage of Instances of the Minority Class (%MIN.), and the Source (Ref.).

ID.	Name	#INST.	#FEA.	#CL.	%MIS.	%MAJ.	%MIN.	Ref.
bnk	Banknote authentication	1372	4	2	0	76.24	23.76	[Dua and Graff 2017]
can	Cancer	569	30	2	0	62.74	37.26	<sup>4</sup>
car	Car acceptance prediction	50	4	2	0	68.00	32.00	<sup>5</sup>
col	Column 3C weka	310	6	3	0	46.13	7.74	[Dua and Graff 2017]
dbt	Diabetes	768	8	2	0	65.10	34.90	[Dua and Graff 2017]
ecl	Ecoli	336	7	8	0	42.86	1.49	[Dua and Graff 2017]
frt	Fruit	898	34	7	0	22.72	7.24	[Koklu et al. 2021a]
gls	Glass	214	9	6	0	35.51	2.34	[Dua and Graff 2017]
hrt	Heart disease	303	13	2	0	54.46	45.54	[Dua and Graff 2017]
hpt	Hepatitis	155	19	2	5.67	79.35	20.65	[Dua and Graff 2017]
hcl	Horse colic	368	22	2	23.80	62.77	37.23	[Dua and Graff 2017]
irs	Iris	150	4	3	0	33.33	33.33	[Dua and Graff 2017]
lnd	Land mines	338	3	5	0	21.01	19.23	[Dua and Graff 2017]
mam	Mammographic masses	961	5	2	3.37	53.69	46.31	[Dua and Graff 2017]
pdy	Paddy leaf	6000	3	4	0	25.00	25.00	<sup>6</sup>
pis	Pistachio	2148	16	2	0	57.36	42.64	[Singh et al. 2022]
pha	Pharyngitis in children	676	18	2	1.86	54.88	45.12	<sup>7</sup>
pre	Predicting response based on engagement KPIs	5000	3	3	0	33.34	33.32	<sup>8</sup>
pmp	Pumpkin	2499	12	2	0	52.00	48.00	[Koklu et al. 2021b]
rsn	Raisin	900	7	2	0	50.00	50.00	[Çinar et al. 2020]
seg	Segment	2310	19	7	0	14.29	14.29	[Dua and Graff 2017]
sir	Sirtuin6 small molecules	100	6	2	0	50.00	50.00	[Dua and Graff 2017]
smk	Smoker condition	1023	7	2	0.20	60.51	30.49	<sup>9</sup>
tae	Teaching assistant evaluation	151	5	3	0	34.44	32.45	[Dua and Graff 2017]
tip	Travel insurance prediction	1987	8	2	0	64.27	35.73	<sup>10</sup>
tit	Titanic	891	6	2	3.31	61.62	38.38	<sup>11</sup>
wne	Wine	178	13	3	0	39.89	26.97	[Dua and Graff 2017]
wbc	Wisconsin breast cancer	699	9	2	0.25	65.52	34.48	[Dua and Graff 2017]
wpb	Wisconsin prognostic breast cancer	198	33	2	0.06	76.26	23.74	[Dua and Graff 2017]
yst	Yeast	1484	8	10	0	31.20	0.34	[Dua and Graff 2017]

and Garrell-Guiu 2003] and [Orriols-Puig et al. 2009]. In UCS, the *unordered bound hyperrectangular representation* [Stone and Bull 2003] is utilized for the rule antecedents. The uniform crossover is used for UCS and Fuzzy-UCS<sub>\*</sub> in the GA. We use our own implementation of UCS and Fuzzy-UCS<sub>\*</sub>, both codified in Julia [Bezanson et al. 2017].

To evaluate the impact of learning duration, we conduct experiments with two different training durations: a shorter duration of 10 epochs to simulate a situation with limited computation resources, and an extended duration of 50 epochs to ensure adequate learning time. Here, an epoch refers to the process where the system trains on the entire training dataset once.

We conduct 30 independent runs for each experiment, each initialized with a different random seed. The datasets are divided using shuffle-split cross-validation, allocating 90% of the instances for training and the remaining 10% for testing, as in [Preen et al. 2021]. All attribute values in the datasets are normalized to the range [0, 1]. The performance metric used to evaluate the systems is the average macro F1 scores, obtained from 30 runs of both the training and test data.

To analyze statistical significance, we first apply the Friedman test to the results of 30 runs on all four systems to determine a significance probability. If the Friedman test indicates a probability

<sup>12</sup>In the context of L(F)CSs, the ruleset size has two distinct definitions [Urbanowicz and Moore 2015]. The first definition is the *micro*-ruleset size, which represents the sum of all rule numerosities in  $[P]$ , calculated as  $\sum_{k \in [P]} \text{num}^k$ . The second definition is the *macro*-ruleset size, which represents the number of unique rules (called macro-rules) currently in  $[P]$ .

Table 2. Properties of the Hyperparameter Values.

Description	Hyperparameter	UCS	Fuzzy-UCS <sub>s</sub>
Maximum micro-ruleset size <sup>12</sup>	$N$	2000	2000
Accuracy threshold	$\text{acc}_0$	0.99	N/A
Fitness threshold	$F_0$	N/A	0.99
Learning rate	$\beta$	0.2	N/A
Fitness exponent	$\nu$	1	1
Crossover probability	$\chi$	0.8	0.8
Mutation probability	$p_{\text{mut}}$	0.04	0.04
Fraction of mean fitness for rule deletion	$\delta$	0.1	0.1
Maximum change amount for mutation	$m_0$	0.1	N/A
Maximum range for covering	$r_0$	1.0	N/A
Time threshold for GA application in [C]	$\theta_{\text{GA}}$	50	50
Experience threshold for rule deletion	$\theta_{\text{del}}$	50	50
Experience threshold for subsumption	$\theta_{\text{sub}}$	50	50
Experience threshold for class inference	$\theta_{\text{exploit}}$	N/A	10
Tournament size	$\tau$	0.4	0.4
Probability of <i>Don't Care</i> symbol in covering	$P_{\#}$	0.33	0.33
Whether correct set subsumption is performed	<i>doCorrectSetSubsumption</i>	yes	yes
Whether GA subsumption is performed	<i>doGASubsumption</i>	yes	yes

small enough, we then proceed with the Holm test, using the Wilcoxon signed-rank test as a post-hoc method. A difference is considered significant if the probability is less than 0.05 in both the Friedman and Holm post-hoc tests.

## 6.2 Results

Tables 3 and 4 present each system's average training and test macro F1 scores and average rank across all datasets At the 10th and 50th epochs, respectively. Green-shaded values denote the best values among all systems, while peach-shaded values indicate the worst values among all systems. The terms "Rank" and "Position" denote each system's overall average rank obtained by using the Friedman test and its position in the final ranking, respectively. Statistical results of the Wilcoxon signed-rank test are summarized with symbols wherein "+", "-", and "~" represent that the macro F1 score of a conventional system is significantly better, worse, and competitive compared to that obtained by the proposed Fuzzy-UCS<sub>DS</sub>, respectively. The "*p*-value" and "*p*<sub>Holm</sub>-value" are derived from the Wilcoxon signed-rank test and the Holm-adjusted Wilcoxon signed-rank test, respectively. Arrows denote whether the rank improved or declined compared to Fuzzy-UCS<sub>DS</sub>. † (††) indicates statistically significant differences compared to Fuzzy-UCS<sub>DS</sub>, i.e., *p*-value (*p*<sub>Holm</sub>-value) <  $\alpha = 0.05$ .

Based on Tables 3 and 4, Fuzzy-UCS<sub>DS</sub> recorded significantly higher test macro F1 scores than all other systems at both the 10th epoch (*p*<sub>Holm</sub> < 0.05) and 50th epoch when compared to Fuzzy-UCS<sub>VOTE</sub> (*p* < 0.05) and Fuzzy-UCS<sub>SWIN</sub> (*p*<sub>Holm</sub> < 0.05), as well as higher average ranks than UCS. Furthermore, Tables 3 and 4 reveal that Fuzzy-UCS<sub>DS</sub> did not register the lowest macro F1 scores for any problem regardless of the number of training epochs, except for the *smk* and *tit* problems in training and test macro F1 scores at the 10th epoch. These findings underscore that Fuzzy-UCS<sub>DS</sub> is a robust system, consistently exhibiting high classification performance across a diverse range of problems.

Additional experimental results are provided in Appendices C-G. In Appendix C, Fuzzy-UCS<sub>DS</sub> demonstrated significantly higher test classification accuracy compared to UCS, Fuzzy-UCS<sub>VOTE</sub>, and Fuzzy-UCS<sub>SWIN</sub>. In Appendix D, Fuzzy-UCS<sub>DS</sub> demonstrated superior performance in artificial noiseless problems compared to Fuzzy-UCS<sub>VOTE</sub> and Fuzzy-UCS<sub>SWIN</sub>. For larger-scale datasets

Table 3. Results When the Number of Training Iterations is 10 Epochs, Displaying Average Macro F1 Scores Across 30 Runs.

10 Epochs	TRAINING MACRO F1 (%)				TEST MACRO F1 (%)			
	UCS	Fuzzy-UCS <sub>VOTE</sub>	Fuzzy-UCS <sub>SWIN</sub>	Fuzzy-UCS <sub>DS</sub>	UCS	Fuzzy-UCS <sub>VOTE</sub>	Fuzzy-UCS <sub>SWIN</sub>	Fuzzy-UCS <sub>DS</sub>
bnk	70.02 -	89.44 -	91.83 +	89.88	68.96 -	89.00 -	91.27 +	89.54
can	93.53 ~	93.26 -	93.37 ~	93.40	89.13 -	92.68 ~	92.82 ~	92.68
car	72.72 -	78.28 -	78.64 ~	79.91	58.31 ~	60.76 ~	61.61 ~	62.35
col	50.65 ~	58.00 +	53.29 ~	51.89	46.96 ~	53.36 +	48.01 ~	48.66
dbt	56.90 ~	59.90 -	56.39 -	60.30	54.91 ~	56.13 ~	53.56 -	56.32
ec1	39.15 -	52.26 -	49.49 -	53.30	36.60 -	56.93 ~	54.78 ~	56.75
frt	81.85 +	75.94 -	73.43 -	80.41	72.96 ~	71.68 -	69.32 -	75.35
gls	40.08 -	40.62 -	52.92 +	47.53	33.67 ~	32.35 ~	40.35 ~	38.49
hrt	82.88 -	88.02 -	89.40 ~	89.31	76.09 -	80.98 ~	80.02 ~	81.58
hpt	84.67 +	74.06 -	75.50 ~	75.05	52.96 -	59.68 ~	59.31 ~	60.27
hc1	74.67 +	62.85 -	61.57 -	64.54	57.25 +	49.90 ~	45.71 -	50.98
irs	74.90 -	93.66 -	94.05 ~	94.38	70.10 -	92.71 ~	93.56 ~	92.93
lnd	32.84 -	20.63 -	24.57 -	35.81	26.89 ~	25.89 ~	23.65 -	28.65
mam	79.71 -	80.32 -	77.12 -	80.45	78.95 ~	78.57 ~	75.93 -	78.84
pdv	72.86 +	34.78 -	34.87 -	38.92	71.90 +	34.81 -	35.12 -	39.30
pis	85.21 -	86.26 ~	84.60 -	86.24	84.05 -	85.44 ~	83.42 -	85.23
pha	75.77 ~	74.85 -	77.88 +	76.25	58.27 -	63.59 ~	61.91 ~	63.08
pre	99.33 ~	99.64 ~	100.0 +	99.60	99.32 ~	99.68 ~	100.0 +	99.60
pmp	86.40 ~	86.78 ~	86.32 -	86.74	85.24 ~	85.98 ~	85.63 -	86.04
rsn	79.90 -	83.53 -	85.11 +	84.26	81.33 -	82.97 -	84.86 +	84.04
seg	87.68 -	88.52 -	88.90 ~	88.95	87.18 -	87.92 -	88.34 -	88.43
sir	70.97 -	83.49 ~	83.89 ~	83.48	67.48 -	79.44 ~	77.42 ~	79.34
smk	84.54 +	71.95 +	83.42 +	67.57	83.73 +	71.17 +	82.71 +	67.28
tae	52.43 -	55.85 -	59.12 -	60.49	42.60 -	44.46 -	47.79 -	51.23
tip	76.30 ~	76.20 ~	74.62 -	76.23	74.40 ~	75.00 ~	72.84 -	74.88
tit	64.56 +	60.55 ~	62.72 +	60.39	65.41 +	61.34 ~	62.31 ~	60.82
wne	87.67 -	97.19 -	97.54 ~	97.61	81.85 -	94.96 ~	93.52 ~	95.34
wbc	95.28 -	96.08 -	95.20 -	96.26	94.26 -	95.81 ~	93.61 -	95.48
wpb	76.83 -	77.56 -	86.74 +	82.61	50.21 ~	53.13 ~	52.19 ~	53.00
yst	32.08 -	38.65 -	41.62 -	43.79	25.36 -	31.95 ~	36.58 ~	36.45
Rank	2.93 <sup>↓†</sup>	2.77 <sup>↓††</sup>	2.40 <sup>↓</sup>	1.90	3.20 <sup>↓††</sup>	2.32 <sup>↓††</sup>	2.63 <sup>↓††</sup>	1.85
Position	4	3	2	1	4	2	3	1
+/-/~	6/17/7	2/22/6	8/13/9	-	4/15/11	2/7/21	4/10/16	-
<i>p</i> -value	0.0327	0.000928	0.360	-	0.00322	0.0332	0.00578	-
<i>p</i> <sub>Holm</sub> -value	0.0654	0.00278	0.360	-	0.00967	0.0332	0.0116	-

(Appendix E), Fuzzy-UCS<sub>DS</sub> maintains stable performance regardless of dataset size, demonstrating its robustness and scalability. Appendix F revealed the following findings: (i) Fuzzy-UCS\* generated significantly fewer rules compared to both UCS and a state-of-the-art nonfuzzy LCS (i.e., scikit-ExSTraCS [Urbanowicz and Moore 2015]); (ii) while scikit-ExSTraCS achieved higher test accuracy on many datasets, Fuzzy-UCS<sub>DS</sub> offers unique advantages in terms of interpretability and simplicity; and (iii) future work will explore incorporating scikit-ExSTraCS's noise-handling mechanisms into Fuzzy-UCS<sub>DS</sub> to further enhance its capabilities. In comparisons with modern classification methods (Appendix G), Random Forest and XGBoost achieved better predictive performance on many datasets than Fuzzy-UCS<sub>DS</sub>, demonstrating a clear trade-off: while these methods offer superior classification accuracy, they lead to significantly higher model complexity.

### 6.3 Discussion

**6.3.1 Comparison With the UCS Nonfuzzy-Classifier System.** Table 3 shows that during the initial learning phase (i.e., after the 10th epoch), UCS recorded the lowest ranks in terms of training and test macro F1 scores. This lower performance can be attributed to the complexity of optimizing non-linguistic rules in UCS. Each dimension in the UCS rule antecedent is represented by two

Table 4. Results When the Number of Training Iterations is 50 Epochs, Displaying Average Macro F1 Scores Across 30 Runs.

50 Epochs	TRAINING MACRO F1 (%)				TEST MACRO F1 (%)			
	UCS	Fuzzy-UCS <sub>VOTE</sub>	Fuzzy-UCS <sub>SWIN</sub>	Fuzzy-UCS <sub>DS</sub>	UCS	Fuzzy-UCS <sub>VOTE</sub>	Fuzzy-UCS <sub>SWIN</sub>	Fuzzy-UCS <sub>DS</sub>
bnk	94.84 +	92.55 -	93.56 +	92.87	94.30 +	92.21 -	92.87 ~	92.51
can	96.98 +	94.83 -	94.31 -	94.95	91.00 -	94.12 ~	93.79 ~	94.17
car	75.85 -	85.22 ~	85.08 ~	85.58	58.10 ~	64.60 ~	63.02 ~	61.92
col	66.28 +	62.95 +	56.13 -	59.76	57.78 ~	59.23 +	52.04 -	55.78
dbt	73.76 +	70.11 ~	62.46 -	70.07	67.66 ~	66.44 ~	57.81 -	66.16
ecl	59.77 -	70.47 ~	65.33 -	69.62	55.93 -	66.03 ~	58.65 -	66.00
frt	91.93 +	82.79 -	80.06 -	84.71	76.60 -	77.87 -	74.15 -	80.58
gls	58.00 -	66.95 ~	65.51 -	67.73	41.58 -	53.82 ~	53.59 ~	54.87
hrt	90.42 -	94.60 -	94.28 -	94.99	80.36 ~	81.13 ~	82.20 ~	81.09
hpt	89.93 -	91.22 -	89.48 -	92.12	51.99 -	62.03 ~	59.07 ~	62.72
hcl	88.73 +	84.13 -	79.55 -	84.84	59.28 ~	59.25 ~	53.48 -	59.18
irs	82.57 -	94.85 -	95.54 ~	95.30	78.11 -	93.29 ~	94.12 ~	93.51
lnd	52.80 +	22.41 -	24.01 -	37.41	36.27 +	25.97 ~	23.61 -	29.55
mam	82.99 +	80.84 -	77.42 -	81.02	80.49 ~	79.55 ~	76.20 -	79.86
pdy	89.18 +	35.73 -	36.09 -	41.93	88.20 +	35.79 -	36.42 -	42.43
pis	87.22 +	86.55 ~	84.77 -	86.56	85.74 ~	85.49 ~	83.86 -	85.52
pha	78.51 -	81.39 -	86.59 +	85.23	60.98 -	65.36 +	63.61 -	64.64
pre	99.63 ~	98.00 -	100.0 +	99.76	99.64 ~	98.03 -	100.0 +	99.79
pmp	87.21 ~	86.91 ~	86.78 -	86.95	85.94 ~	85.99 ~	85.84 -	86.04
rsn	84.97 ~	84.19 -	85.47 +	85.05	84.49 ~	83.86 -	85.06 ~	84.80
seg	95.42 +	89.69 -	90.05 -	90.07	92.90 +	89.18 -	89.25 ~	89.68
sir	76.28 -	84.70 ~	84.93 ~	84.69	68.41 -	80.19 ~	79.70 ~	80.44
smk	97.59 +	95.07 -	92.88 -	95.42	96.38 +	94.61 ~	92.46 -	94.66
tae	58.07 -	62.95 -	63.59 ~	63.84	46.55 -	51.19 ~	51.41 -	53.22
tip	79.69 +	77.16 -	76.03 -	77.26	76.83 +	75.57 ~	73.98 -	75.79
tit	68.82 ~	68.48 ~	63.29 -	68.42	68.11 ~	68.00 ~	62.38 -	68.08
wne	93.72 +	98.33 -	98.59 -	98.79	88.25 -	96.01 ~	95.44 ~	96.16
wbc	97.32 +	96.81 ~	95.99 -	96.76	95.73 ~	95.74 ~	94.66 -	95.46
wpb	93.22 +	86.89 -	90.44 +	88.69	54.80 ~	56.16 ~	53.64 ~	55.71
yst	57.47 +	52.15 -	52.69 -	54.56	46.24 ~	45.18 -	45.36 ~	45.75
Rank	2.10↓	2.90↓ <sup>††</sup>	2.97↓ <sup>††</sup>	2.03	2.50↓	2.47↓ <sup>†</sup>	3.07↓ <sup>††</sup>	1.97
Position	2	3	4	1	3	2	4	1
+/-/~	16/10/4	1/20/9	5/19/6	-	6/10/14	2/6/22	1/12/17	-
$p$ -value	0.821	0.000471	0.000593	-	0.221	0.0368	0.000110	-
$p_{Holm}$ -value	0.821	0.00141	0.00141	-	0.221	0.0736	0.000331	-

continuous values defining the matching interval's lower and upper bounds. In contrast, Fuzzy-UCS\* employs the pre-specified linguistic terms to discretely partition the input space for each dimension of the rule antecedent, thus reducing the complexity of the search space. Consequently, UCS, with its relatively large rule search space, shows weaker performance than Fuzzy-UCS\* in the early stages of learning.

Conversely, with adequate learning time (i.e., 50 epochs), UCS enhances its training macro F1 scores and demonstrates performance that significantly competes with Fuzzy-UCS<sub>DS</sub>, which recorded the highest rank in training data classification ( $p_{Holm} = 0.821$ , cf. Table 4). Moreover, as evidenced by the results of the Wilcoxon signed-rank test, UCS recorded significantly higher training macro F1 scores compared to Fuzzy-UCS<sub>DS</sub> in 16 problems. This count exceeds the number of problems where Fuzzy-UCS<sub>DS</sub> recorded significantly higher training macro F1 scores compared to UCS, which is 10 problems. This enhancement results from the non-linguistic rules' ability to accurately capture the training data through their capacity to partition the input space arbitrarily. However, the rank of UCS on test data classification remains lower than that of Fuzzy-UCS<sub>VOTE</sub> and Fuzzy-UCS<sub>DS</sub>. This finding aligns with reported experimental results in [Shiraishi et al. 2023], which suggests that nonfuzzy rules tend to overfit training data, thus reducing their effectiveness on unseen test data. Indeed, while UCS shows significantly higher training macro F1 scores than

Fuzzy-UCS<sub>DS</sub> in high-dimensional problems with greater than or equal to 30 dimensions (e.g., *frt*) and problems with missing attributes (e.g., *hpt*), its test macro F1 score is significantly lower.

Thus, in situations characterized by inherent uncertainty, such as real-world classification problems, fuzzy systems like Fuzzy-UCS<sub>DS</sub> demonstrate greater efficacy than nonfuzzy systems like UCS. However, it is worth noting that linguistic rules might not always be advantageous, especially in cases like the *pdy* problem where all attributes are continuous, and more specific rules are required for accurate classification [Shiraishi et al. 2022].

**6.3.2 Impact of the DS Theory-based Class Inference Scheme.** As shown in Tables 3 and 4, Fuzzy-UCS<sub>DS</sub> demonstrates a consistent improvement in training and test macro F1 scores from the initial learning phase (10 epochs) to the later learning phase (50 epochs) across many datasets. This tendency reveals that the DS theory-based inference scheme becomes more effective as the learning progresses and the system’s fuzzy rules are further optimized. While Fuzzy-UCS<sub>DS</sub> already shows effective performance in the initial learning phase with limited rule optimization (i.e., after 10 epochs), its capability is notably enhanced when more epochs for rule adjustment is allowed (i.e., 50 epochs). The observed slight decrease in the average ranking of Fuzzy-UCS<sub>DS</sub> from 10 to 50 epochs does not indicate a decline in performance. This can be attributed to the improvement of some other systems in the later learning phase. Unlike Fuzzy-UCS<sub>DS</sub>, UCS and the other two Fuzzy-UCS\* variants may require a more comprehensive set of well-adjusted rules to achieve high performance. On the other hand, Fuzzy-UCS<sub>DS</sub> can efficiently utilize less-adjusted rules in the initial learning phase and continues to perform robustly as the rules become more adjusted in the later learning phase.

A key strength of Fuzzy-UCS<sub>DS</sub> is its capacity to mitigate “false overconfidence” in class inference, especially when it is based on uncertain training data. This is achieved by quantitatively expressing uncertainty (i.e., the “I don’t know” state) through the complete ignorance hypothesis  $\Theta$ , a fundamental concept of the DS theory. At the same time, Fuzzy-UCS<sub>DS</sub> utilizes the strength of fuzzy rules in reducing overfitting, as noted in [Shiraishi et al. 2023]. This contributes to the improvement of the reliability and accuracy of the classification process. The combination of DS theory’s robustness with the flexibility of fuzzy rules emphasizes the effectiveness of Fuzzy-UCS<sub>DS</sub>. This dual approach is effective in various learning tasks. Notably, in datasets with pronounced class imbalance (e.g., *ecl*, *frt*, *gls*, *yst*), no significant performance degradation was observed for Fuzzy-UCS<sub>DS</sub> at either epoch point compared to other systems. This suggests that Fuzzy-UCS<sub>DS</sub> helps mitigate bias introduced by class imbalance, leveraging its ability to capture uncertain (i.e., class-imbalanced) information through the DS theory, as discussed in [Tian et al. 2022].

**6.3.3 Complexity of Each Class Inference Scheme.** In the context of L(F)CSs, complexity is often defined by the number of rules within the system [Liu et al. 2021]. From this perspective, there is no difference in complexity among the Fuzzy-UCS variants—Fuzzy-UCS<sub>VOTE</sub>, Fuzzy-UCS<sub>SWIN</sub>, and Fuzzy-UCS<sub>DS</sub>—as they all utilize the same ruleset generated during training, that is, they do not affect the rule generation process.

However, when considering the prediction-level complexity, differences arise:

- **Voting-based inference (Fuzzy-UCS<sub>VOTE</sub>):** This scheme typically results in moderate complexity due to its reliance on aggregating votes from multiple rules. It provides a good balance between computational efficiency and robustness by leveraging collective decision-making but may not handle uncertainty as effectively as more complex schemes. Our results indicate that Fuzzy-UCS<sub>VOTE</sub> is inferior to Fuzzy-UCS<sub>DS</sub> in terms of average rank in test macro F1 scores (cf. Section 6.2)

- **Single-winner-based inference (Fuzzy-UCS<sub>SWIN</sub>):** This scheme generally has lower complexity as it selects a single rule with the highest fitness for decision-making. However, it may sacrifice robustness due to its reliance on individual rule performance. Our results indicate that Fuzzy-UCS<sub>SWIN</sub> is inferior to Fuzzy-UCS<sub>VOTE</sub> and Fuzzy-UCS<sub>DS</sub> in terms of average rank in test macro F1 scores (cf. Section 6.2).
- **DS theory-based inference (Fuzzy-UCS<sub>DS</sub>):** This scheme tends to have higher complexity due to its comprehensive approach to uncertainty management. It requires calculating and combining belief masses, which adds computational layers but enhances robustness and interpretability by providing confidence measures for decisions. Our results indicate that Fuzzy-UCS<sub>DS</sub> is superior to Fuzzy-UCS<sub>VOTE</sub> and Fuzzy-UCS<sub>SWIN</sub> in terms of average rank in test macro F1 scores (cf. Section 6.2), but takes longer runtime than Fuzzy-UCS<sub>VOTE</sub> and Fuzzy-UCS<sub>SWIN</sub> (cf. Section 7.1).

In conclusion, while the rule-level complexity remains consistent across these schemes, the choice of inference scheme should be guided by the specific requirements of the application domain. For tasks that demand high interpretability and robustness, such as in healthcare or finance, the Fuzzy-UCS<sub>DS</sub> scheme offers significant advantages despite its higher complexity. The ability to quantify uncertainty and provide confidence measures can be crucial in these sensitive domains. Conversely, applications with strict computational constraints or real-time processing requirements might benefit more from simpler schemes like Fuzzy-UCS<sub>SWIN</sub>, which offers faster decision-making at the expense of some robustness.

## 7 ANALYSIS

This section further provides analytical results: Section 7.1 presents the runtime comparisons; Section 7.2 examines the characteristics of decision boundaries provided by each class inference scheme; Section 7.3 explains how to interpret the inference results acquired by Fuzzy-UCS<sub>DS</sub>; and Section 7.4 quantifies the “I don’t know” state in Fuzzy-UCS<sub>DS</sub>.

### 7.1 Runtime Comparisons

We conduct runtime comparisons to assess the computational efficiency of the proposed DS theory-based class inference scheme (Fuzzy-UCS<sub>DS</sub>). Specifically, we compare the runtimes of UCS and each variant of Fuzzy-UCS<sub>\*</sub>. All experiments are conducted using our implementations in Julia, on an Intel® Core™ i7-9700 CPU at 3.00 GHz with 16 GB RAM, following the experimental setup outlined in Section 6.1.

Table 5 presents the runtime required to complete one run for UCS and each variant of Fuzzy-UCS<sub>\*</sub> at the 10th and 50th epochs. Green-shaded values indicate the best (shortest) runtimes, while peach-shaded values denote the worst (longest) runtimes.

As shown in Table 5, Fuzzy-UCS<sub>DS</sub> recorded the longest runtime among all systems at both the 10th and 50th epochs. Specifically, compared to Fuzzy-UCS<sub>VOTE</sub> and Fuzzy-UCS<sub>SWIN</sub>, Fuzzy-UCS<sub>DS</sub> required approximately 1.5 to 2 times longer to complete. This increase in runtime is attributable to the computational complexity introduced by the DS theory-based inference mechanism, particularly

Table 5. Average Runtime to Complete One Run.

RUNTIME (SEC.)							
10 Epochs				50 Epochs			
UCS	Fuzzy-UCS <sub>VOTE</sub>	Fuzzy-UCS <sub>SWIN</sub>	Fuzzy-UCS <sub>DS</sub>	UCS	Fuzzy-UCS <sub>VOTE</sub>	Fuzzy-UCS <sub>SWIN</sub>	Fuzzy-UCS <sub>DS</sub>
1.478	3.214	3.147	7.174	9.113	49.93	49.26	73.33

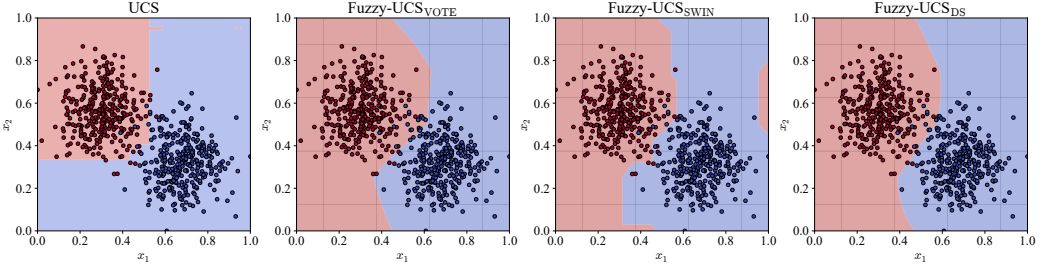


Fig. 4. Decision boundaries obtained with UCS and Fuzzy-UCS\*. UCS, Fuzzy-UCS<sub>VOTE</sub>, Fuzzy-UCS<sub>SWIN</sub>, and Fuzzy-UCS<sub>DS</sub> achieved 94.65 %, 96.84%, 97.45%, and 97.74% average training accuracy, respectively.

when the number of hypotheses (i.e., class labels) is large. This complexity represents a notable limitation of our approach. Furthermore, nonfuzzy systems such as UCS demonstrated significantly shorter runtimes compared to their fuzzy counterparts like Fuzzy-UCS. This difference is primarily due to the necessity in fuzzy systems to calculate membership degrees for each rule every time the match set  $[M]$  is formed, which serves as a computational bottleneck.

While Fuzzy-UCS<sub>DS</sub> offers significant improvements in classification performance, its increased runtime is an important consideration. Future work may explore optimization techniques to mitigate this computational cost, thereby enhancing the practicality of the DS theory-based inference scheme in real-world applications.

## 7.2 Visualization of Decision Boundaries

This subsection aims to visually analyze the decision boundaries formed by each system. We use an artificial dataset generated by *scikit-learn* [Pedregosa et al. 2011] for a comparative experiment. As depicted in Fig. 4, the dataset comprises a class-balanced binary classification problem with a total of 600 two-dimensional data points. Data points from class  $c_1$  are shown in blue and class  $c_2$  in red. This problem is difficult for UCS with interval-based nonfuzzy rules and also for Fuzzy-UCS\* with linguistic fuzzy rules because it involves some noisy data points and requires curved decision boundaries for effective classification. The system configuration aligns with the experiment in Section 6, and the number of training iterations is set to 10 epochs.

Fig. 4 illustrates the inferred class assignments  $\hat{c} \in \{c_1, c_2\}$  by each system in the input space, shown in blue and red, respectively (resolution:  $1000 \times 1000$ ). For Fuzzy-UCS\*, the grid in each plot indicates the  $5 \times 5$  partition of the input space by the intersection points of the adjacent membership functions for the five linguistic terms. Note again that all three Fuzzy-UCS\* variants use the same  $[P]$ . The training accuracy achieved is detailed in the figure captions, representing averages across 30 runs with different seeds. A randomly selected run among the 30 runs is selected for visualization in Fig. 4.

The decision boundaries offer several insights:

- UCS only creates boundaries that are axis-parallel.
- Fuzzy-UCS<sub>VOTE</sub> forms a slightly smooth, oblique boundary due to the collective voting of multiple rules.
- Fuzzy-UCS<sub>SWIN</sub> presents a steeper boundary than Fuzzy-UCS<sub>VOTE</sub> since it relies on a single rule with the highest  $\mu_{A^k}(\mathbf{x}) \cdot F^k$  for inference. This leads to potentially unintuitive class assignments in subregions lacking training data, such as around (1.0, 0.6). Some parts of the boundary are axis-parallel as in UCS, while others are non-axis-parallel as in Fuzzy-UCS<sub>VOTE</sub>.

- Fuzzy-UCS<sub>DS</sub> exhibits the highest training accuracy among all four systems. This is attributed to the combination of belief masses from multiple rules across different hypotheses (i.e.,  $\{\theta_1\}$ ,  $\{\theta_2\}$ ,  $\Theta$ ) using Dempster's rule of combination. The smoothest boundary is obtained by Fuzzy-UCS<sub>DS</sub> among the four systems in Fig. 4.

### 7.3 Visualization of Belief Masses for Each Hypothesis

This subsection aims to visually interpret the inference results by Fuzzy-UCS<sub>DS</sub>. We use an artificial dataset in Fig. 5, which is inspired from [Masson and Dencœux 2008]. As shown in Fig. 5, the dataset is a binary classification problem with 25 data points: including 13 blue (class  $c_1$ ) and 12 red (class  $c_2$ ) data points. No data points are given in the top and bottom regions where  $x_2 \in [0.0, 0.25)$  and  $x_2 \in (0.75, 1.0]$ . On the vertical line with  $x_1 = 0.5$ , three blue points and two red points are given. The 25 data points show the perfect symmetry with respect to the horizontal line with  $x_2 = 0.5$ . The setup for Fuzzy-UCS<sub>DS</sub> and the training epochs remain the same as in Section 7.2.

Fig. 5 displays class assignments  $\hat{c} \in \{c_1, c_2\}$  by Fuzzy-UCS<sub>DS</sub> and belief mass landscapes for each hypothesis ( $m_{[M]}(\{\theta_1\})$ ,  $m_{[M]}(\{\theta_2\})$ ,  $m_{[M]}(\Theta)$ ). The color in each belief mass figure shows the value of the belief mass at the corresponding point in the input space (i.e., the darker color shows the larger value of the belief mass, and the zero belief mass is shown by white color). As explained in Section 4, the sum of the belief mass values over the three figures is always 1 at any point in the input space. The landscape for  $m_{[M]}(\Theta)$  is shown on a logarithmic scale for clarity. The average training accuracy by Fuzzy-UCS<sub>DS</sub> is 91.33% over 30 runs with different seeds. A randomly selected run among the 30 runs is selected for visualization in Fig. 5.

The results show that Fuzzy-UCS<sub>DS</sub> forms a smooth vertical class boundary, correctly classifying all training data, except for those along the line of  $x_1 = 0.5$ . Investigating the belief mass landscape provides several insights:

- In subregions close to the training data, the values for the "I don't know" belief mass,  $m_{[M]}(\Theta)$ , are close to 0. This is because Fuzzy-UCS\* activates the covering operator which ensures that the sum of correct answer rules' membership degrees is always greater than 1 (cf. Alg. 1, line 8). As a result, total membership degrees in the neighborhood of training data points tend to be high. Consequently, this leads to low values of  $m_{[M]}(\Theta)$  in these areas.
- In the two subregions with no data points (i.e.,  $x_2 \leq 0.2$  and  $x_2 > 0.8$ ), the function value of  $m_{[M]}(\Theta)$  is large. This indicates greater uncertainty due to fewer rules covering these subregions.
- In the challenging subregion with mixed classes (around  $x_1 = 0.5$ ),  $m_{[M]}(\{\theta_1\})$  and  $m_{[M]}(\{\theta_2\})$  are close to 0.5, and  $m_{[M]}(\Theta)$  is close to 0. This reflects the presence of rules that equally support conflicting hypotheses.
- In simpler subregions (e.g., around  $(0.0, 0.5)$  and  $(1.0, 0.5)$ ), where classification is easy,  $m_{[M]}(\Theta)$  is close to 0, and a high belief mass is observed for a specific class hypothesis.

In a nutshell, the belief masses across all hypotheses help interpret the inference result  $\hat{c}$ :

- In subregions where  $m_{[M]}(\Theta)$  is close to 0, and only one specific class hypothesis has a high belief mass, classification by fuzzy rules is easy. Hence,  $\hat{c}$  is likely to be correct.
- In subregions where  $m_{[M]}(\Theta)$  is close to 0 and several specific class hypotheses have similar belief masses, classification by fuzzy rules is difficult. Hence,  $\hat{c}$  may be unreliable. Those subregions are likely around the class boundary.
- In subregions where  $m_{[M]}(\Theta)$  is close to 1, it is unclear whether classification by fuzzy rules is easy or difficult. Hence, the reliability of  $\hat{c}$  is uncertain. Those subregions likely have no training data points.

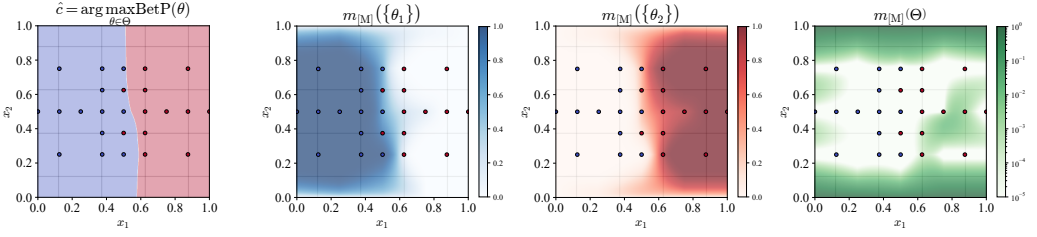


Fig. 5. Class assignments  $\hat{c} \in \{c_1, c_2\}$  by Fuzzy-UCS<sub>DS</sub> and belief mass landscapes for each hypothesis:  $m_{[M]}(\{\theta_1\})$ : class  $c_1$ ,  $m_{[M]}(\{\theta_2\})$ : class  $c_2$ ,  $m_{[M]}(\Theta)$ : complete ignorance (“I don’t know”). All figures are a result of a randomly selected run.

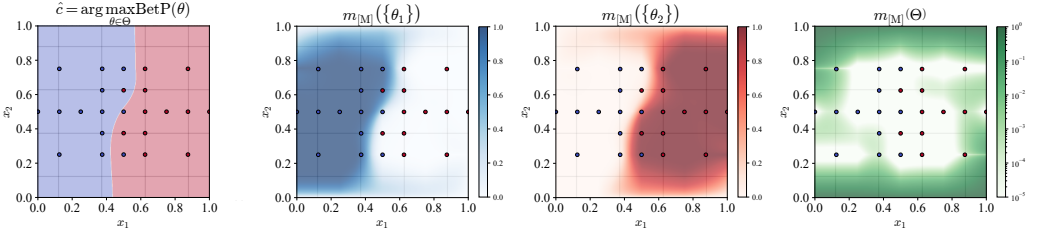


Fig. 6. Class assignments by Fuzzy-UCS<sub>DS</sub> and belief mass landscapes for each hypothesis. All figures are a result of a single run that has the worst training accuracy.

This analysis demonstrates how the belief mass function for each hypothesis can provide insights into the confidence and uncertainty associated with these classifications.

In Fig. 5, we can observe that each result (e.g., classification boundary in the left-most figure) is not symmetric with respect to the horizontal line with  $x_1 = 0.5$ . This is because the fuzzy rule generation in Fuzzy-UCS depends on the presentation order of the given training data points. Whereas slightly different results are obtained from different runs with different seeds, we can always obtain the above-mentioned observation. In Fig. 6, we show the results of a single run that has the worst training data accuracy 88.00%. We can see that similar belief mass functions are obtained in Figs. 5 and 6.

#### 7.4 Quantification of the “I Don’t Know” State

The DS theory-based class inference scheme assigns a belief mass to the “I don’t know” state when high uncertainty is detected during classification. This subsection reports the belief mass associated with the “I don’t know” state for all data points in both the training and test datasets., providing insights into how our approach manages uncertainty. A higher “I don’t know” belief mass indicates greater uncertainty in classification. Therefore, it is expected that Fuzzy-UCS<sub>DS</sub> will output a higher “I don’t know” belief mass on test datasets, which contain unseen data points, compared to training datasets. The experimental setup adheres to the conditions outlined in Section 6.1.

Table 6 presents the average “I don’t know” belief mass,  $m_{\mathcal{D}}(\Theta)$ , at the 5th, 10th, and 50th epochs, where:

$$m_{\mathcal{D}}(\Theta) = \frac{\sum_{\mathbf{x} \in \mathcal{D}} m_{[M]}(\Theta; \mathbf{x})}{|\mathcal{D}|}, \quad (20)$$

Table 6. Results Displaying Average “I Don’t Know” Belief Mass Across 30 Runs.

	$m_{\mathcal{D}}(\Theta)$ : “I DON’T KNOW”					
	5 Epochs		10 Epochs		50 Epochs	
	Training	Test	Training	Test	Training	Test
bnk	0.8017	0.8031 ~	0.9789	0.9751 ~	0.9803	0.9797 ~
can	0.04141	0.04784 ~	0.01276	0.02871 -	0.004121	0.02284 -
car	0.008148	0.03333 ~	0.0007407	0.01333 ~	0.4407	0.4400 ~
col	0.4514	0.4516 ~	0.7001	0.7054 ~	0.9781	0.9731 ~
dbt	0.6629	0.6727 ~	0.9413	0.9377 ~	0.9253	0.9238 ~
ecl	0.2845	0.2767 ~	0.5311	0.5069 ~	0.6077	0.5912 ~
frt	0.02212	0.02273 ~	0.02679	0.02785 ~	0.01153	0.01357 ~
gls	0.6045	0.5971 ~	0.7670	0.7857 ~	0.6359	0.6486 ~
hrt	0.01391	0.01516 ~	0.03634	0.03578 ~	0.005305	0.01687 -
hpt	0.1381	0.1910 -	0.05583	0.09489 -	0.01826	0.09713 -
hcl	0.07774	0.1428 -	0.06792	0.1420 -	0.03079	0.1549 -
irs	3.582E-5	1.785E-5 +	0.006181	0.01111 -	0.5249	0.5200 ~
lnd	0.9798	0.9775 ~	0.9969	0.9961 ~	0.9332	0.9500 -
mam	0.7961	0.8007 ~	0.9832	0.9845 ~	0.9902	0.9900 ~
pdy	0.9013	0.9035 ~	0.7812	0.7861 -	0.5905	0.5924 ~
pis	0.6408	0.6411 ~	0.8007	0.7964 ~	0.8232	0.8200 ~
pha	0.06045	0.06271 ~	0.01429	0.01767 ~	0.009177	0.03297 -
pre	0.9790	0.9805 -	0.9559	0.9566 ~	0.9984	0.9983 ~
pmp	0.7902	0.7963 ~	0.9206	0.9235 ~	0.9626	0.9629 ~
rsn	0.6606	0.6600 ~	0.9004	0.8978 ~	0.9807	0.9811 ~
seg	0.1223	0.1236 ~	0.05225	0.04753 ~	0.01814	0.01998 ~
sir	0.003658	0.007363 ~	0.001045	0.002416 ~	0.4744	0.4567 ~
smk	0.9926	0.9919 ~	0.9971	0.9971 ~	0.9982	0.9987 ~
tae	0.04667	0.05208 ~	0.4225	0.4062 ~	0.8256	0.8021 ~
tip	0.8788	0.8628 +	0.8550	0.8509 ~	0.5107	0.5104 ~
tit	0.9784	0.9767 ~	0.9994	0.9978 ~	0.9967	0.9948 ~
wne	0.02619	0.03305 ~	0.007416	0.01272 ~	0.03417	0.04105 ~
wbc	0.01929	0.01897 ~	0.08151	0.07905 ~	0.07059	0.07000 ~
wpb	0.3321	0.4033 -	0.07253	0.2628 -	0.04257	0.2831 -
yst	0.9981	0.9978 ~	0.4002	0.4096 ~	0.1602	0.1636 ~
Rank	1.33	1.67 $\downarrow$ <sup>†</sup>	1.42	1.58 $\downarrow$	1.47	1.53 $\downarrow$
Position	1	2	1	2	1	2
+/-/~	-	2/4/24	-	0/6/24	-	0/7/23
<i>p</i> -value	-	0.0285	-	0.137	-	0.245

and  $\mathcal{D} \in \{\mathcal{D}_{tr}, \mathcal{D}_{te}\}$  represents a training or test dataset. Green-shaded values denote the smallest (best) values between the “I don’t know” belief mass from a training dataset and that from a test dataset. These values represent the degree of uncertainty in classification, ranging from 0 (complete certainty) to 1 (complete uncertainty), rather than the proportion of “I don’t know” predictions. For example, a value of 0.8017 for the bnk dataset at the 5th epoch during training means that, on average, 80.17% of the total belief mass was assigned to the “I don’t know” state when classifying data points in this training dataset, indicating high uncertainty in Fuzzy-UCS<sub>DS</sub>’s predictions. Note that even with high “I don’t know” belief mass, Fuzzy-UCS<sub>DS</sub> still makes class predictions based on the remaining belief mass distributed among specific classes through the pignistic transform (cf. Section 4.4). Statistical results from the Wilcoxon signed-rank test are summarized with symbols wherein “+”, “-”, and “~” represent that the “I don’t know” belief mass from a test dataset is significantly smaller, larger, or competitive compared to that from a training dataset, respectively. The “*p*-value” is derived from the Wilcoxon signed-rank test. Arrows denote whether the rank improved or declined compared to the “I don’t know” belief mass from a training dataset. † indicates statistically significant differences compared to the “I don’t know” belief mass from a training dataset, i.e., *p*-value <  $\alpha = 0.05$ .

From Table 6, it is evident that at the 5th, 10th, and 50th epochs, the average rank during testing is lower than during training, meaning that Fuzzy-UCS<sub>DS</sub> tends to output a larger “I don’t know” belief

mass during testing than during training. Particularly at the 5th epoch, there was a statistically significant difference in the “I don’t know” belief mass between training and testing ( $p < 0.05$ ). At the 10th and 50th epochs, as expected, there were no datasets where the “I don’t know” belief mass during testing was significantly smaller than during training (denoted by the “+” symbol). An interesting insight is that the seven datasets showing a significantly larger “I don’t know” belief mass during testing at the 50th epoch (i.e., can, hrt, hpt, hc1, lnd, pha, and wpb, denoted by the “-” symbol) were all characterized by high uncertainty, i.e., either having very small instance counts (676 or fewer) and/or containing missing values. These results, along with analyses from Section 7.3, conclude that the “I don’t know” belief mass output by Fuzzy-UCS<sub>DS</sub> adequately quantifies classification uncertainty.

## 8 CONCLUDING REMARKS

This article introduced a novel class inference scheme for LFCSs, using the DS theory to enhance LFCS performance, especially in uncertain real-world problem domains. Our scheme transforms the membership degrees and weight vectors of multiple fuzzy rules into belief mass functions. These belief mass functions are then integrated using Dempster’s rule of combination and the pignistic transform during the class inference process. The application of the proposed inference scheme within the Fuzzy-UCS framework yielded significant improvement in classification performance on real-world problems. A key advantage of our scheme is its ability to provide both inference results and a measure of confidence for each inference result. This offers valuable insights into the certainty of classification.

Future research directions include:

- Applying our DS theory-based class inference scheme to recently studied XCSR [Wagner and Stein 2022] and ACS2 [Smierzchała et al. 2023] classifier systems for reinforcement learning tasks with discrete action labels (e.g., an action label set is {up, down, left, right}).
- Extending our scheme to various evolutionary learning algorithms that generate sets of solutions, each suggesting different classifications for a given input (e.g., multi-tree Genetic Programming [Fan et al. 2024]).
- Extending our scheme to LFCSs which can deal with multi-label classification problems (e.g., [Omozaki et al. 2022]) by developing a methodology that accounts for belief mass assignment to meta-classes.
- Exploring the combined application of our scheme and *absumption* techniques [Liu et al. 2023, 2024; Shiraishi et al. 2022]. Investigating whether these two techniques complement each other or exhibit redundancy will provide deeper insights into optimizing LFCS architectures for enhanced generalization and robustness against overfitting.
- Addressing limitations of the use of predefined fuzzy sets (e.g., our homogeneous linguistic discretization of domain intervals), such as the potential imposition of assumptions about data distribution [Antonelli et al. 2009] and the loss of specificity in some domains where precision is essential [Orriols-Puig et al. 2009]. This could involve integrating adaptive discretization methods [Murata and Ishibuchi 1995] that adjust linguistic term partitions to feature distributions and/or mixed discrete-continuous attribute list knowledge representation [Urbanowicz and Moore 2015] that handles both discrete and continuous attributes effectively.
- Investigating the application of the DS theory in Pittsburgh-style LFCSs, which often result in more compact rule sets and may enhance interpretability and efficiency. Comparisons with existing work (e.g., [Bishop et al. 2021]) could provide valuable insights.

- Developing benchmark datasets to evaluate LFCS capabilities by incorporating characteristics such as inherent linguistic uncertainty, interpretability-focused problems, and varying degrees of feature overlap.

## ACKNOWLEDGMENTS

This work was supported by the Japan Society for the Promotion of Science KAKENHI (Grant Nos. JP23KJ0993, JP23K20388), the National Natural Science Foundation of China (Grant No. 62376115), and the Guangdong Provincial Key Laboratory (Grant No. 2020B121201001).

## REFERENCES

- Amina Adadi and Mohammed Berrada. 2018. Peeking Inside the Black-Box: A Survey on Explainable Artificial Intelligence (XAI). *IEEE Access* 6 (2018), 52138–52160. <https://doi.org/10.1109/ACCESS.2018.2870052>
- Sneha Aenugu and Lee Spector. 2019. Lexicase selection in learning classifier systems. In *Proceedings of the Genetic and Evolutionary Computation Conference (Prague, Czech Republic) (GECCO '19)*. Association for Computing Machinery, New York, NY, USA, 356–364. <https://doi.org/10.1145/3321707.3321828>
- Michela Antonelli, Pietro Ducange, Beatrice Lazzarini, and Francesco Marcelloni. 2009. Multi-objective evolutionary learning of granularity, membership function parameters and rules of Mamdani fuzzy systems. *Evolutionary Intelligence* 2 (2009), 21–37. <https://doi.org/10.1007/s12065-009-0022-3>
- Andras Bardossy and Lucien Duckstein. 1995. Fuzzy Rule-Based Modeling with Applications to Geophysical, Biological, and Engineering Systems. <https://doi.org/10.1201/9780138755133>
- Fatiha Belmahdi, Mourad Lazri, Fethi Ouallouche, Karim Labadi, Rafik Absi, and Soltane Ameer. 2023. Application of Dempster-Shafer theory for optimization of precipitation classification and estimation results from remote sensing data using machine learning. *Remote Sensing Applications: Society and Environment* 29 (2023), 100906. <https://doi.org/10.1016/j.rsase.2022.100906>
- Ester Bernadó-Mansilla and Josep M. Garrell-Guiu. 2003. Accuracy-Based Learning Classifier Systems: Models, Analysis and Applications to Classification Tasks. *Evolutionary Computation* 11, 3 (sep 2003), 209–238. <https://doi.org/10.1162/106365603322365289>
- Malcolm Beynon, Darren Cosker, and David Marshall. 2001. An expert system for multi-criteria decision making using Dempster Shafer theory. *Expert Systems with Applications* 20, 4 (2001), 357–367. [https://doi.org/10.1016/S0957-4174\(01\)00020-3](https://doi.org/10.1016/S0957-4174(01)00020-3)
- Jeff Bezanson, Alan Edelman, Stefan Karpinski, and Viral B. Shah. 2017. Julia: A Fresh Approach to Numerical Computing. *SIAM Rev.* 59, 1 (2017), 65–98. <https://doi.org/10.1137/141000671>
- James C Bezdek. 2013. *Pattern recognition with fuzzy objective function algorithms*. Springer Science & Business Media. <https://doi.org/10.1007/978-1-4757-0450-1>
- Jordan T. Bishop, Marcus Gallagher, and Will N. Browne. 2021. A genetic fuzzy system for interpretable and parsimonious reinforcement learning policies. In *Proceedings of the Genetic and Evolutionary Computation Conference Companion (Lille, France) (GECCO '21)*. Association for Computing Machinery, New York, NY, USA, 1630–1638. <https://doi.org/10.1145/3449726.3463198>
- Bernhard E. Boser, Isabelle M. Guyon, and Vladimir N. Vapnik. 1992. A training algorithm for optimal margin classifiers. In *Proceedings of the Fifth Annual Workshop on Computational Learning Theory (Pittsburgh, Pennsylvania, USA) (COLT '92)*. Association for Computing Machinery, New York, NY, USA, 144–152. <https://doi.org/10.1145/130385.130401>
- Leo Breiman. 2001. Random forests. *Machine Learning* 45 (2001), 5–32. <https://doi.org/10.1023/A:1010933404324>
- M.V. Butz, T. Kovacs, P.L. Lanzi, and S.W. Wilson. 2004. Toward a theory of generalization and learning in XCS. *IEEE Trans. Evol. Comput.* 8, 1 (Feb 2004), 28–46. <https://doi.org/10.1109/TEVC.2003.818194>
- Jorge Casillas, Brian Carse, and Larry Bull. 2007. Fuzzy-XCS: A Michigan Genetic Fuzzy System. *IEEE Transactions on Fuzzy Systems* 15, 4 (Aug 2007), 536–550. <https://doi.org/10.1109/TFUZZ.2007.900904>
- Tianqi Chen and Carlos Guestrin. 2016. XGBoost: A Scalable Tree Boosting System. In *Proceedings of the 22nd ACM SIGKDD International Conference on Knowledge Discovery and Data Mining (San Francisco, California, USA) (KDD '16)*. Association for Computing Machinery, New York, NY, USA, 785–794. <https://doi.org/10.1145/2939672.2939785>
- İlkay Çınar, Murat Koklu, and Şakir Taşdemir. 2020. Classification of raisin grains using machine vision and artificial intelligence methods. *Gazi Mühendislik Bilimleri Dergisi* 6, 3 (12 2020), 200–209. <https://doi.org/10.30855/gmbd.2020.03.03>
- Arthur P Dempster. 1967. Upper and Lower Probabilities Induced by a Multivalued Mapping. *The Annals of Mathematical Statistics* 38, 2 (1967), 325–339. [https://doi.org/10.1007/978-3-540-44792-4\\_3](https://doi.org/10.1007/978-3-540-44792-4_3)
- Thierry Denceux. 1995. A k-nearest neighbor classification rule based on Dempster-Shafer theory. *IEEE Transactions on Systems, Man, and Cybernetics* 25, 5 (1995), 804–813. <https://doi.org/10.1109/21.376493>

- Dheeru Dua and Casey Graff. 2017. UCI Machine Learning Repository. <http://archive.ics.uci.edu/ml>
- Qinglan Fan, Ying Bi, Bing Xue, and Mengjie Zhang. 2024. Multi-Tree Genetic Programming for Learning Color and Multi-Scale Features in Image Classification. *IEEE Transactions on Evolutionary Computation* (2024), 1–1. <https://doi.org/10.1109/TEVC.2024.3384021>
- Rahma Ferjani, Lilia Rejeb, Chedi Abdelkarim, and Lamjed Ben Said. 2024. Evidential Supervised Classifier System: A New Learning Classifier System Dealing with Imperfect Information. *International Journal of Information Technology & Decision Making* 23, 02 (2024), 917–938. <https://doi.org/10.1142/S0219622022500997>
- Alberto Fernandez, Francisco Herrera, Oscar Cordon, Maria Jose del Jesus, and Francesco Marcelloni. 2019. Evolutionary Fuzzy Systems for Explainable Artificial Intelligence: Why, When, What for, and Where to? *IEEE Computational Intelligence Magazine* 14, 1 (2019), 69–81. <https://doi.org/10.1109/MCI.2018.2881645>
- Zhun ga Liu, Quan Pan, and Jean Dezert. 2013. A new belief-based K-nearest neighbor classification method. *Pattern Recognition* 46, 3 (2013), 834–844. <https://doi.org/10.1016/j.patcog.2012.10.001>
- David Edward Goldberg. 2002. *The design of innovation: Lessons from and for competent genetic algorithms*. Vol. 1. Springer. <https://doi.org/10.1007/978-1-4757-3643-4>
- Thimmaiah Gudiyangada Nachappa, Sepideh Tavakkoli Piralilou, Khalil Gholamnia, Omid Ghorbanzadeh, Omid Rahmati, and Thomas Blaschke. 2020. Flood susceptibility mapping with machine learning, multi-criteria decision analysis and ensemble using Dempster Shafer Theory. *Journal of Hydrology* 590 (2020), 125275. <https://doi.org/10.1016/j.jhydrol.2020.125275>
- Michael AS Guth. 1988. Uncertainty analysis of rule-based expert systems with Dempster-Shafer mass assignments. *International journal of intelligent systems* 3, 2 (1988), 123–139. <https://doi.org/10.1002/int.4550030203>
- Koki Hamasaki and Masaya Nakata. 2021. Minimum Rule-Repair Algorithm for Supervised Learning Classifier Systems on Real-Valued Classification Tasks. In *International Conference on Metaheuristics and Nature Inspired Computing*. Springer, 137–151. [https://doi.org/10.1007/978-3-030-94216-8\\_11](https://doi.org/10.1007/978-3-030-94216-8_11)
- John H Holland. 1986. Escaping Brittleness: The possibilities of general-purpose learning algorithms applied to parallel rule-based systems. *Mach. Learn. Artif. Intell. Approach* 2 (1986), 593–623.
- Dedek Indra Gunawan Hutasuht, Deny Adhar, Erwin Ginting, Andrian Syahputra, et al. 2018. Expert System Detect Stroke with Dempster Shafer Method. In *2018 6th International Conference on Cyber and IT Service Management (CITSM)*. IEEE, 1–4. <https://doi.org/10.1109/CITSM.2018.8674053>
- Muhammad Iqbal, Will N. Browne, and Mengjie Zhang. 2014. Reusing Building Blocks of Extracted Knowledge to Solve Complex, Large-Scale Boolean Problems. *IEEE Trans. Evol. Comput.* 18, 4 (2014), 465–480. <https://doi.org/10.1109/TEVC.2013.2281537>
- Hisao Ishibuchi, Tomoharu Nakashima, and Tadahiko Murata. 1999. Performance evaluation of fuzzy classifier systems for multidimensional pattern classification problems. *IEEE Transactions on Systems, Man, and Cybernetics, Part B (Cybernetics)* 29, 5 (1999), 601–618. <https://doi.org/10.1109/3477.790443>
- Hisao Ishibuchi, Tomoharu Nakashima, and Manabu Nii. 2004. *Classification and modeling with linguistic information granules: Advanced approaches to linguistic Data Mining*. Springer Science & Business Media. <https://doi.org/10.1007/b138232>
- Hisao Ishibuchi and Takashi Yamamoto. 2005. Rule weight specification in fuzzy rule-based classification systems. *IEEE Transactions on Fuzzy Systems* 13, 4 (2005), 428–435. <https://doi.org/10.1109/TFUZZ.2004.841738>
- George H. John and Pat Langley. 1995. Estimating continuous distributions in Bayesian classifiers. In *Proceedings of the Eleventh Conference on Uncertainty in Artificial Intelligence (Montréal, Qué, Canada) (UAI'95)*. Morgan Kaufmann Publishers Inc., San Francisco, CA, USA, 338–345.
- Yousri Kessentini, Thomas Burger, and Thierry Paquet. 2015. A Dempster–Shafer Theory based combination of handwriting recognition systems with multiple rejection strategies. *Pattern Recognition* 48, 2 (2015), 534–544. <https://doi.org/10.1016/j.patcog.2014.08.010>
- Murat Koklu, Ramazan Kursun, Yavuz Selim Taspinar, and Ilkay Cinar. 2021a. Classification of date fruits into genetic varieties using image analysis. *Mathematical Problems in Engineering* 2021 (2021). <https://doi.org/10.1155/2021/4793293>
- Murat Koklu, Seyma Sarigil, and Osman Ozbek. 2021b. The use of machine learning methods in classification of pumpkin seeds (*Cucurbita pepo* L.). *Genetic Resources and Crop Evolution* 68, 7 (2021), 2713–2726. <https://doi.org/10.1007/s10722-021-01226-0>
- Eric Lefevre, Olivier Colot, and Patrick Vannoorenberghe. 2002. Belief function combination and conflict management. *Information Fusion* 3, 2 (2002), 149–162. [https://doi.org/10.1016/S1566-2535\(02\)00053-2](https://doi.org/10.1016/S1566-2535(02)00053-2)
- Jidong Li and Xuejie Zhang. 2024. Construction of fuzzy classification systems by fitness sharing based genetic search and boosting based ensemble. *Fuzzy Sets and Systems* 484 (2024), 108949. <https://doi.org/10.1016/j.fss.2024.108949>
- Mujin Li, Honghui Xu, and Yong Deng. 2019. Evidential decision tree based on belief entropy. *Entropy* 21, 9 (2019), 897. <https://doi.org/10.3390/e21090897>
- Yi Liu, Will N. Browne, and Bing Xue. 2020. Absumption and subsumption based learning classifier systems. In *Proceedings of the 2020 Genetic and Evolutionary Computation Conference (Cancún, Mexico) (GECCO '20)*. Association for Computing Machinery, New York, NY, USA, 368–376. <https://doi.org/10.1145/3377930.3389813>

- Yi Liu, Will N. Browne, and Bing Xue. 2021. Visualizations for rule-based machine learning. *Natural Computing* 21 (2021), 243–264. <https://doi.org/10.1007/s11047-020-09840-0>
- Yi Liu, Yu Cui, Will Browne, Bing Xue, Wen Cheng, Yong Li, and Lingfang Zeng. 2023. Absumption and Subsumption based Learning Classifier System for Real-World Continuous-based Problems. In *Proceedings of the Companion Conference on Genetic and Evolutionary Computation* (Lisbon, Portugal) (GECCO '23 Companion). Association for Computing Machinery, New York, NY, USA, 299–302. <https://doi.org/10.1145/3583133.3590564>
- Yi Liu, Yu Cui, Wen Cheng, Will Neil Browne, Bing Xue, Chengyuan Zhu, Yiding Zhang, Mingkai Sheng, and Lingfang Zeng. 2024. A Phenotypic Learning Classifier System for Problems with Continuous Features. In *Proceedings of the Genetic and Evolutionary Computation Conference* (Melbourne, VIC, Australia) (GECCO '24). Association for Computing Machinery, New York, NY, USA, 349–357. <https://doi.org/10.1145/3638529.3654007>
- Marie-Hélène Masson and T. Denceux. 2008. ECM: An evidential version of the fuzzy c-means algorithm. *Pattern Recognition* 41, 4 (2008), 1384–1397. <https://doi.org/10.1016/j.patcog.2007.08.014>
- Yani Mulyani, Eka Fitrajaya Rahman, Herbert, and Lala Septem Riza. 2016. A new approach on prediction of fever disease by using a combination of Dempster Shafer and Naïve bayes. In *2016 2nd International Conference on Science in Information Technology (ICSITech)*. 367–371. <https://doi.org/10.1109/ICSITech.2016.7852664>
- T. Murata and H. Ishibuchi. 1995. Adjusting membership functions of fuzzy classification rules by genetic algorithms. In *Proceedings of 1995 IEEE International Conference on Fuzzy Systems.*, Vol. 4. 1819–1824 vol.4. <https://doi.org/10.1109/FUZZY.1995.409928>
- Masaya Nakata and Will N. Browne. 2021. Learning Optimality Theory for Accuracy-Based Learning Classifier Systems. *IEEE Transactions on Evolutionary Computation* 25, 1 (2021), 61–74. <https://doi.org/10.1109/TEVC.2020.2994314>
- Yusuke Nojima, Koyo Kawano, Hajime Shimahara, Eric Vernon, Naoki Masuyama, and Hisao Ishibuchi. 2023. Fuzzy Classifiers with a Two-Stage Reject Option. In *2023 IEEE International Conference on Fuzzy Systems (FUZZ-IEEE)*. 1–6. <https://doi.org/10.1109/FUZZ52849.2023.10309729>
- Yusuke Nojima, Kazuhiro Watanabe, and Hisao Ishibuchi. 2015. Simple modifications on heuristic rule generation and rule evaluation in Michigan-style fuzzy genetics-based machine learning. In *2015 IEEE International Conference on Fuzzy Systems (FUZZ-IEEE)*. 1–8. <https://doi.org/10.1109/FUZZ-IEEE.2015.7338115>
- Yuichi Omozaki, Naoki Masuyama, Yusuke Nojima, and Hisao Ishibuchi. 2020. Multiobjective Fuzzy Genetics-Based Machine Learning for Multi-Label Classification. In *2020 IEEE International Conference on Fuzzy Systems (FUZZ-IEEE)*. 1–8. <https://doi.org/10.1109/FUZZ48607.2020.9177804>
- Yuichi Omozaki, Naoki Masuyama, Yusuke Nojima, and Hisao Ishibuchi. 2022. Evolutionary Multi-Objective Multi-Tasking for Fuzzy Genetics-Based Machine Learning in Multi-Label Classification. In *2022 IEEE International Conference on Fuzzy Systems (FUZZ-IEEE)*. 1–8. <https://doi.org/10.1109/FUZZ-IEEE55066.2022.9882681>
- Albert Orriols-Puig and Jorge Casillas. 2011. Fuzzy knowledge representation study for incremental learning in data streams and classification problems. *Soft Computing* 15, 12 (2011), 2389–2414. <https://doi.org/10.1007/s00500-010-0668-x>
- Albert Orriols-Puig, Jorge Casillas, and Ester Bernado-Mansilla. 2009. Fuzzy-UCS: A Michigan-Style Learning Fuzzy-Classifier System for Supervised Learning. *IEEE Transactions on Evolutionary Computation* 13, 2 (2009), 260–283. <https://doi.org/10.1109/TEVC.2008.925144>
- Evandro S. Ortigossa, Thales Gonçalves, and Luis Gustavo Nonato. 2024. EXplainable Artificial Intelligence (XAI)—From Theory to Methods and Applications. *IEEE Access* 12 (2024), 80799–80846. <https://doi.org/10.1109/ACCESS.2024.3409843>
- Fabian Pedregosa, Gaël Varoquaux, Alexandre Gramfort, Vincent Michel, Bertrand Thirion, Olivier Grisel, Mathieu Blondel, Peter Prettenhofer, Ron Weiss, Vincent Dubourg, Jake Vanderplas, Alexandre Passos, David Cournapeau, Matthieu Brucher, Matthieu Perrot, and Édouard Duchesnay. 2011. Scikit-learn: Machine Learning in Python. *J. Mach. Learn. Res.* 12, null (nov 2011), 2825–2830.
- Richard J. Preen, Stewart W. Wilson, and Larry Bull. 2021. Autoencoding With a Classifier System. *IEEE Transactions on Evolutionary Computation* 25, 6 (2021), 1079–1090. <https://doi.org/10.1109/TEVC.2021.3079320>
- J Ross Quinlan. 1993. C4.5: Programs for machine learning. *The Morgan Kaufmann Series in Machine Learning* (1993).
- Omid Rahmati and Assefa M. Melesse. 2016. Application of Dempster-Shafer theory, spatial analysis and remote sensing for groundwater potentiality and nitrate pollution analysis in the semi-arid region of Khuzestan, Iran. *Science of The Total Environment* 568 (2016), 1110–1123. <https://doi.org/10.1016/j.scitotenv.2016.06.176>
- Murat Sensoy, Lance Kaplan, and Melih Kandemir. 2018. Evidential Deep Learning to Quantify Classification Uncertainty. In *Advances in Neural Information Processing Systems*, Vol. 31. Curran Associates, Inc. [https://proceedings.neurips.cc/paper\\_files/paper/2018/file/a981f2b708044d6fb4a71a1463242520-Paper.pdf](https://proceedings.neurips.cc/paper_files/paper/2018/file/a981f2b708044d6fb4a71a1463242520-Paper.pdf)
- Glenn Shafer. 1976. *A mathematical theory of evidence*. Vol. 42. Princeton university press.
- Hiroki Shiraiishi, Yohei Hayamizu, and Tomonori Hashiyama. 2023. Fuzzy-UCS Revisited: Self-Adaptation of Rule Representations in Michigan-Style Learning Fuzzy-Classifier Systems. In *Proceedings of the Genetic and Evolutionary Computation Conference* (Lisbon, Portugal) (GECCO '23). Association for Computing Machinery, New York, NY, USA, 548–557. <https://doi.org/10.1145/3583131.3590360>

- Hiroki Shiraishi, Yohei Hayamizu, Hiroyuki Sato, and Keiki Takadama. 2022. Absumption based on overgenerality and condition-clustering based specialization for XCS with continuous-valued inputs. In *Proceedings of the Genetic and Evolutionary Computation Conference* (Boston, Massachusetts) (GECCO '22). Association for Computing Machinery, New York, NY, USA, 422–430. <https://doi.org/10.1145/3512290.3528841>
- Hiroki Shiraishi, Hisao Ishibuchi, and Masaya Nakata. 2025. Evidential Fuzzy Rule-Based Machine Learning to Quantify Classification Uncertainty. *Authorea Preprints* (2025). <https://doi.org/10.36227/techrxiv.174900814.43483543/v1>
- Farzaneh Shoeleh, Ali Hamzeh, and Sattar Hashemi. 2011. Towards final rule set reduction in XCS: a fuzzy representation approach. In *Proceedings of the 13th Annual Conference on Genetic and Evolutionary Computation* (Dublin, Ireland) (GECCO '11). Association for Computing Machinery, New York, NY, USA, 1211–1218. <https://doi.org/10.1145/2001576.2001740>
- Dilbag Singh, Yavuz Selim Taspinar, Ramazan Kursun, Ilkay Cinar, Murat Koklu, Ilker Ali Ozkan, and Heung-No Lee. 2022. Classification and Analysis of Pistachio Species with Pre-Trained Deep Learning Models. *Electronics* 11, 7 (2022). <https://doi.org/10.3390/electronics11070981>
- Philippe Smets. 1990. The combination of evidence in the transferable belief model. *IEEE Transactions on Pattern Analysis and Machine Intelligence* 12, 5 (1990), 447–458. <https://doi.org/10.1109/34.55104>
- Philippe Smets. 2000. Data fusion in the transferable belief model. In *Proceedings of the third international conference on information fusion*, Vol. 1. IEEE, PS21–PS33. <https://doi.org/10.1109/IFIC.2000.862713>
- Philippe Smets. 2005. Decision making in the TBM: the necessity of the pignistic transformation. *International journal of approximate reasoning* 38, 2 (2005), 133–147. <https://doi.org/10.1016/j.ijar.2004.05.003>
- Philippe Smets and Robert Kennes. 1994. The transferable belief model. *Artificial Intelligence* 66, 2 (1994), 191–234. [https://doi.org/10.1016/0004-3702\(94\)90026-4](https://doi.org/10.1016/0004-3702(94)90026-4)
- Łukasz Smierzchała, Norbert Kozłowski, and Olgierd Unold. 2023. Anticipatory Classifier System With Episode-Based Experience Replay. *IEEE Access* 11 (2023), 41190–41204. <https://doi.org/10.1109/ACCESS.2023.3269879>
- Christopher Stone and Larry Bull. 2003. For Real! XCS with Continuous-Valued Inputs. *Evolutionary Computation* 11, 3 (sep 2003), 299–336. <https://doi.org/10.1162/106365603322365315>
- Masakazu Tadokoro, Hiroyuki Sato, and Keiki Takadama. 2021. XCS with Weight-based Matching in VAE Latent Space and Additional Learning of High-Dimensional Data. In *2021 IEEE Congress on Evolutionary Computation (CEC)*. 304–310. <https://doi.org/10.1109/CEC45853.2021.9504909>
- Asitha Thumapati and Yan Zhang. 2023. Towards Optimizing Performance of Machine Learning Algorithms on Unbalanced Dataset. *Artificial Intelligence & Applications* (2023). <https://doi.org/10.5121/csit.2023.131914>
- Hongpeng Tian, Zuowei Zhang, Arnaud Martin, and Zhunga Liu. 2022. Reliability-Based Imbalanced Data Classification with Dempster-Shafer Theory. In *International Conference on Belief Functions*. Springer, 77–86. [https://doi.org/10.1007/978-3-031-17801-6\\_8](https://doi.org/10.1007/978-3-031-17801-6_8)
- Fani A. Tzima and Pericles A. Mitkas. 2013. Strength-based learning classifier systems revisited: Effective rule evolution in supervised classification tasks. *Engineering Applications of Artificial Intelligence* 26, 2 (2013), 818–832. <https://doi.org/10.1016/j.engappai.2012.09.022>
- Ryan John Urbanowicz and Jason H Moore. 2015. ExSTraCS 2.0: description and evaluation of a scalable learning classifier system. *Evolutionary intelligence* 8, 2 (2015), 89–116. <https://doi.org/10.1007/s12065-015-0128-8>
- Manuel Valenzuela-Rendón. 1991. The fuzzy classifier system: Motivations and first results. In *Parallel Problem Solving from Nature*. Springer Berlin Heidelberg, Berlin, Heidelberg, 338–342. <https://doi.org/10.1007/BFb0029774>
- Alexander R. M. Wagner and Anthony Stein. 2022. Mechanisms to Alleviate Over-Generalization in XCS for Continuous-Valued Input Spaces. *SN Computer Science* 3, 2 (2022), 1–23. <https://doi.org/10.1007/s42979-022-01060-w>
- Stewart W. Wilson. 1995. Classifier Fitness Based on Accuracy. *Evolutionary Computation* 3, 2 (jun 1995), 149–175. <https://doi.org/10.1162/evco.1995.3.2.149>
- Stewart W Wilson. 1998. Generalization in the XCS Classifier System. *Proceedings of the Third Annual Genetic Programming Conference (GP-98)* (1998).
- Stewart W Wilson. 1999. Get real! XCS with continuous-valued inputs. In *Int. Worksh. Learn. Classif. Syst.* Springer, 209–219.
- Alexa Woodward, Harsh Bandhey, Jason H. Moore, and Ryan J. Urbanowicz. 2024. Survival-LCS: A Rule-Based Machine Learning Approach to Survival Analysis. In *Proceedings of the Genetic and Evolutionary Computation Conference* (Melbourne, VIC, Australia) (GECCO '24). Association for Computing Machinery, New York, NY, USA, 431–439. <https://doi.org/10.1145/3638529.3654154>
- Ronald R. Yager. 1987. On the dempster-shafer framework and new combination rules. *Information Sciences* 41, 2 (1987), 93–137. [https://doi.org/10.1016/0020-0255\(87\)90007-7](https://doi.org/10.1016/0020-0255(87)90007-7)
- Ronald R Yager and Liping Liu. 2008. *Classic works of the Dempster-Shafer theory of belief functions*. Vol. 219. Springer. [https://doi.org/10.1007/978-3-540-44792-4\\_1](https://doi.org/10.1007/978-3-540-44792-4_1)
- Navid Moshtaghi Yazdani. 2020. Diagnosing soft tissue sub-surface masses using the XCS classification system. *Frontiers in Health Informatics* 9, 1 (2020), 49. <https://doi.org/10.30699/fhi.v9i1.239>

- Lotfi Asker Zadeh. 1975. The concept of a linguistic variable and its application to approximate reasoning—I. *Information sciences* 8, 3 (1975), 199–249. [https://doi.org/10.1016/0020-0255\(75\)90036-5](https://doi.org/10.1016/0020-0255(75)90036-5)
- Robert Zhang, Rachael Stolzenberg-Solomon, Shannon M. Lynch, and Ryan J. Urbanowicz. 2021. LCS-DIVE: An Automated Rule-based Machine Learning Visualization Pipeline for Characterizing Complex Associations in Classification. arXiv:2104.12844 [cs.LG]
- Qifeng Zhou, Hao Zhou, Qingqing Zhou, Fan Yang, Linkai Luo, and Tao Li. 2015. Structural damage detection based on posteriori probability support vector machine and Dempster–Shafer evidence theory. *Applied Soft Computing* 36 (2015), 368–374. <https://doi.org/10.1016/j.asoc.2015.06.057>

## A ANALYSIS OF FITNESS RANGE IMPACT

A notable feature of Fuzzy-UCS is the use of a fitness range of  $(-1, 1]$ , which differs from the traditional  $(0, 1]$  range used in many classifier systems. This extended range was originally introduced by Ishibuchi and Yamamoto [2005], who demonstrated its effectiveness in improving the performance of LFCSs. Following their findings, the original Fuzzy-UCS paper [Orriols-Puig et al. 2009] adopted this extended range as the default setting.

To validate the effectiveness of the  $(-1, 1]$  fitness range in our Fuzzy-UCS variants, we conduct comparative experiments, where the same problems and experimental settings as in Section 6.1 are used. The number of training iterations is set to 50 epochs. Here, fitness values within the  $(0, 1]$  range have been calculated according to Ishibuchi and Yamamoto's original formulation:  $F_{t+1}^k = \max(v_{t+1}^k)$ .

Table 7 presents the training and test classification accuracy for each variant of Fuzzy-UCS<sub>\*</sub> at the 50th epoch. Green-shaded values denote the best values between Fuzzy-UCS<sub>\*</sub> with a fitness range of  $(-1, 1]$  and Fuzzy-UCS<sub>\*</sub> with a fitness range of  $(0, 1]$ . Statistical results of the Wilcoxon signed-rank test are summarized with symbols wherein “+”, “-”, and “~” represent that the classification accuracy of Fuzzy-UCS<sub>\*</sub> with a fitness range of  $(0, 1]$  is significantly better, worse, and competitive compared to that obtained by Fuzzy-UCS<sub>\*</sub> with a fitness range of  $(-1, 1]$ , respectively. The “*p*-value”

Table 7. Results When Changing Fitness Ranges, Displaying Average Classification Accuracy Across 30 Runs.

$F^k \in$	TRAINING ACCURACY (%)						TEST ACCURACY (%)					
	Fuzzy-UCS <sub>VOTE</sub>		Fuzzy-UCS <sub>SWIN</sub>		Fuzzy-UCS <sub>DS</sub>		Fuzzy-UCS <sub>VOTE</sub>		Fuzzy-UCS <sub>SWIN</sub>		Fuzzy-UCS <sub>DS</sub>	
	$(-1, 1]$	$(0, 1]$	$(-1, 1]$	$(0, 1]$	$(-1, 1]$	$(0, 1]$	$(-1, 1]$	$(0, 1]$	$(-1, 1]$	$(0, 1]$	$(-1, 1]$	$(0, 1]$
bnk	92.63	91.86 -	93.65	91.92 -	92.95	91.94 -	92.34	91.40 -	93.00	91.86 -	92.63	91.43 -
can	95.29	95.29 ~	94.83	94.94 ~	95.39	95.12 -	94.74	94.44 ~	94.44	94.09 ~	94.80	94.68 ~
car	87.93	85.04 -	88.07	88.37 ~	88.22	88.44 ~	76.00	74.67 ~	76.67	75.33 ~	74.00	77.33 ~
col	71.85	68.58 -	68.24	65.90 -	71.37	67.31 -	69.35	66.77 ~	65.81	64.84 ~	69.03	65.59 -
dbt	76.36	77.07 +	73.57	70.62 -	76.48	75.05 -	73.07	74.29 +	70.04	66.97 -	72.94	72.21 ~
ec1	85.79	87.34 +	80.39	78.32 -	85.64	83.63 -	84.02	86.08 +	79.80	77.94 ~	83.92	83.43 ~
frt	87.12	88.14 +	85.17	85.80 +	88.43	88.26 ~	84.74	86.30 +	82.33	83.26 ~	86.44	86.11 ~
gls	72.01	68.63 -	71.75	69.25 -	72.14	66.55 -	62.73	59.09 -	64.09	61.67 ~	64.39	55.45 -
hrt	94.66	93.27 -	94.35	93.97 ~	95.05	94.08 -	81.83	82.69 ~	82.69	82.69 ~	81.83	82.58 ~
hpt	91.46	90.22 -	89.88	88.75 -	92.33	90.86 -	64.58	63.33 ~	62.08	63.75 ~	65.62	63.96 ~
hc1	87.25	87.69 ~	84.19	83.72 ~	87.76	86.58 -	71.80	70.00 ~	69.37	71.17 ~	71.62	68.83 -
irs	94.81	94.02 ~	95.51	95.65 ~	95.26	94.84 ~	94.00	93.11 ~	94.89	94.44 ~	94.22	92.89 ~
lnd	32.05	45.01 +	39.18	42.03 +	46.27	49.41 +	38.24	32.35 -	40.10	40.59 ~	40.20	34.12 -
mam	80.89	80.61 -	77.89	77.87 ~	81.07	80.94 ~	79.73	80.10 ~	76.77	76.63 ~	80.03	79.90 ~
pdv	50.94	68.48 +	50.70	51.93 +	53.94	72.40 +	51.46	68.56 +	51.36	52.54 +	54.63	71.83 +
pis	86.89	86.64 -	85.53	84.54 -	86.91	86.73 -	85.88	86.08 ~	84.67	83.29 -	85.92	85.84 ~
pha	82.10	77.95 -	86.80	83.95 -	85.64	83.22 -	66.96	67.45 ~	64.41	63.73 ~	66.13	67.01 ~
pre	98.01	98.69 +	100.0	100.0 ~	99.76	99.98 +	98.03	98.87 +	100.0	100.0 ~	99.79	100.0 +
pmp	86.99	86.97 ~	86.89	86.10 -	87.03	86.93 -	86.17	85.97 ~	86.05	85.40 -	86.21	85.95 ~
rsn	84.33	84.43 ~	85.51	85.56 ~	85.13	84.79 ~	84.19	84.44 ~	85.30	85.30 ~	85.07	84.81 ~
seg	90.10	89.45 -	90.52	91.01 +	90.42	90.19 -	89.88	89.25 -	90.01	90.85 +	90.30	89.73 ~
sir	84.78	83.52 -	85.00	82.93 -	84.78	83.89 -	81.67	79.00 ~	81.33	80.00 ~	82.00	81.00 ~
smk	95.39	93.15 -	93.49	62.81 -	95.71	86.73 -	95.08	93.11 -	93.14	63.01 -	95.11	86.76 -
tae	63.63	59.70 -	64.15	62.77 ~	64.35	60.59 -	54.58	55.00 ~	53.75	55.00 ~	56.46	55.42 ~
tip	81.09	80.77 ~	80.24	79.33 ~	81.20	80.87 ~	80.00	79.87 ~	78.88	78.21 -	80.23	80.00 ~
tit	72.28	71.64 -	70.57	69.21 -	72.38	71.86 -	71.30	70.85 ~	68.93	67.96 ~	71.52	71.07 ~
wne	98.31	97.65 ~	98.58	98.23 ~	98.79	98.00 -	96.48	96.67 ~	96.11	94.63 ~	96.67	97.41 ~
wbc	97.12	97.23 ~	96.42	96.50 ~	97.07	97.15 ~	96.19	96.38 ~	95.29	95.10 ~	95.95	96.14 ~
wpb	91.57	91.46 ~	93.60	93.73 ~	92.58	91.93 -	72.17	74.33 ~	71.67	71.83 ~	72.00	73.50 ~
yst	53.26	49.62 -	56.22	49.18 -	58.78	45.86 -	52.04	49.40 ~	53.65	48.43 -	57.61	45.86 -
Rank	1.32	1.68↓	1.35	1.65↓†	1.17	1.83↓†	1.47	1.53↓	1.32	1.68↓†	1.27	1.73↓†
Position	1	2	1	2	1	2	1	2	1	2	1	2
+/-/~	-	6/17/7	-	4/14/12	-	3/20/7	-	5/4/21	-	2/7/21	-	2/7/21
<i>p</i> -value	-	0.0645	-	0.00599	-	0.000743	-	0.329	-	0.0385	-	0.0341

is derived from the Wilcoxon signed-rank test. Arrows denote whether the rank improved or declined compared to Fuzzy-UCS\* with a fitness range of  $(-1, 1]$ . † indicates statistically significant differences compared to Fuzzy-UCS\* with a fitness range of  $(-1, 1]$ , i.e.,  $p$ -value  $< \alpha = 0.05$ .

The experimental results show that the use of  $(-1, 1]$  fitness range improved the test accuracy of Fuzzy-UCS\* with the  $(0, 1]$  fitness range on many datasets, as evidenced by lower average ranks in the table. Negative fitness values allow the system to assign penalties to rules that have a high probability of misclassifying instances. In LFCs including Fuzzy-UCS, rules with negative fitness values are excluded from parent selection in the GA (refer to Section 3.2.1). This mechanism enables the GA to guide the system in systematically eliminating inaccurate rules, thereby enhancing the performance of the classifier.

## B ANALYSIS OF EXPERIENCE UPDATE METHODS

In traditional LCSs such as UCS, the experience of a rule is typically updated incrementally as the match set is formed, using the formula  $\exp_{t+1}^k = \exp_t^k + 1$ . This approach uniformly increases the experience of all matched rules by one at each time step, regardless of their individual contributions to the classification process. In contrast, Fuzzy-UCS introduces a membership degree-based experience update method:  $\exp_{t+1}^k = \exp_t^k + \mu_{A^k}(\mathbf{x})$ . This approach updates experience based on membership degrees, allowing rules that are more relevant to the input data to receive greater experience increments. This differentiation enables the GA to prioritize and evolve rules that have higher contributions to accurate classification.

To examine the impact of these different methods of updating experience on the classification performance of Fuzzy-UCS, we conduct comparative experiments, where the same problems and experimental settings as in Section 6.1 are used. The number of training iterations is set to 50 epochs.

Table 8 presents the training and test classification accuracy for each variant of Fuzzy-UCS<sub>\*</sub> at the 50th epoch. Green-shaded values denote the best values between Fuzzy-UCS<sub>\*</sub> with the  $\exp_{t+1}^k = \exp_t^k + \mu_{A^k}(\mathbf{x})$  update method (denoted as Fuzzy-UCS<sub>\*</sub>-Memb) and Fuzzy-UCS<sub>\*</sub> with

Table 8. Results When Changing Experience Update Method, Displaying Average Classification Accuracy Across 30 Runs.

$\exp_{t+1}^k = \exp_t^k +$	TRAINING ACCURACY (%)						TEST ACCURACY (%)					
	Fuzzy-UCS <sub>VOTE</sub>		Fuzzy-UCS <sub>SWIN</sub>		Fuzzy-UCS <sub>DS</sub>		Fuzzy-UCS <sub>VOTE</sub>		Fuzzy-UCS <sub>SWIN</sub>		Fuzzy-UCS <sub>DS</sub>	
	$\mu_{A^k}(\mathbf{x})$	1	$\mu_{A^k}(\mathbf{x})$	1	$\mu_{A^k}(\mathbf{x})$	1	$\mu_{A^k}(\mathbf{x})$	1	$\mu_{A^k}(\mathbf{x})$	1	$\mu_{A^k}(\mathbf{x})$	1
bnk	92.63	55.53 –	93.65	52.96 –	92.95	55.53 –	92.34	55.63 –	93.00	52.87 –	92.63	55.63 –
can	95.29	62.74 –	94.83	61.92 –	95.39	62.74 –	94.74	62.75 –	94.44	61.64 –	94.80	62.75 –
car	87.93	68.22 –	88.07	68.22 –	88.22	68.22 –	76.00	66.00 –	76.67	66.00 –	74.00	66.00 –
col	71.85	23.94 –	68.24	47.84 –	71.37	48.40 –	69.35	23.23 –	65.81	47.96 –	69.03	48.28 –
dbt	76.36	65.24 –	73.57	65.24 –	76.48	65.24 –	73.07	63.90 –	70.04	63.90 –	72.94	63.90 –
ec1	85.79	20.52 –	80.39	41.61 –	85.64	42.24 –	84.02	20.59 –	79.80	44.51 –	83.92	45.39 –
frt	87.12	7.550 –	85.17	20.59 –	88.43	22.35 –	84.74	7.148 –	82.33	22.22 –	86.44	19.78 –
gls	72.01	7.726 –	71.75	34.51 –	72.14	35.75 –	62.73	9.848 –	64.09	32.42 –	64.39	31.67 –
hrt	94.66	54.52 –	94.35	51.73 –	95.05	54.52 –	81.83	53.87 –	82.69	49.35 –	81.83	53.87 –
hpt	91.46	54.87 –	89.88	52.33 –	92.33	54.87 –	64.58	54.58 –	62.08	51.67 –	65.62	54.58 –
hc1	87.25	66.07 –	84.19	65.18 –	87.76	66.07 –	71.80	68.38 –	69.37	65.59 ~	71.62	68.38 –
irs	94.81	32.15 –	95.51	33.70 –	95.26	34.57 –	94.00	44.00 –	94.89	30.00 –	94.22	22.22 –
lnd	32.05	19.41 –	39.18	19.85 –	46.27	21.17 –	38.24	21.37 –	40.10	19.61 –	40.20	16.47 –
mam	80.89	53.73 –	77.89	51.13 –	81.07	53.73 –	79.73	53.33 –	76.77	49.73 –	80.03	53.33 –
pdy	50.94	24.83 –	50.70	24.94 –	53.94	25.17 –	51.46	26.51 –	51.36	25.54 –	54.63	23.44 –
pis	86.89	57.39 –	85.53	55.44 –	86.91	57.39 –	85.88	57.07 –	84.67	54.96 –	85.92	57.07 –
pha	82.10	55.09 –	86.80	51.60 –	85.64	55.09 –	66.96	53.04 –	64.41	51.86 –	66.13	53.04 –
pre	98.01	33.22 –	100.0	33.22 –	99.76	33.49 –	98.03	34.37 –	100.0	34.36 –	99.79	31.88 –
pmp	86.99	51.91 –	86.89	50.08 –	87.03	51.91 –	86.17	52.80 –	86.05	50.59 –	86.21	52.80 –
rsn	84.33	50.54 –	85.51	49.86 –	85.13	50.54 –	84.19	45.15 –	85.30	51.30 –	85.07	45.15 –
seg	90.10	14.10 –	90.52	14.23 –	90.42	14.49 –	89.88	15.99 –	90.01	14.76 –	90.30	12.42 –
sir	84.78	51.56 –	85.00	50.81 –	84.78	51.56 –	81.67	36.00 –	81.33	42.67 –	82.00	36.00 –
smk	95.39	60.46 –	93.49	58.30 –	95.71	60.46 –	95.08	60.91 –	93.14	59.32 –	95.11	60.91 –
tae	63.63	31.98 –	64.15	33.04 –	64.35	35.04 –	54.58	42.92 –	53.75	33.12 –	56.46	25.00 –
tip	81.09	64.18 –	80.24	64.18 –	81.20	64.18 –	80.00	65.09 –	78.88	65.09 –	80.23	65.09 –
tit	72.28	61.77 –	70.57	61.77 –	72.38	61.77 –	71.30	60.22 –	68.93	60.22 –	71.52	60.22 –
wne	98.31	29.35 –	98.58	35.94 –	98.79	40.08 –	96.48	32.22 –	96.11	31.67 –	96.67	38.15 –
wbc	97.12	65.57 –	96.42	65.57 –	97.07	65.57 –	96.19	65.05 –	95.29	65.05 –	95.95	65.05 –
wpb	91.57	76.29 –	93.60	76.29 –	92.58	76.29 –	72.17	76.00 +	71.67	76.00 +	72.00	76.00 +
ybt	53.26	15.53 –	56.22	28.80 –	58.78	31.15 –	52.04	16.06 –	53.65	28.10 –	57.61	31.66 –
Rank	1.00	2.00 <sup>†</sup>	1.00	2.00 <sup>†</sup>	1.00	2.00 <sup>†</sup>	1.03	1.97 <sup>†</sup>	1.03	1.97 <sup>†</sup>	1.03	1.97 <sup>†</sup>
Position	1	2	1	2	1	2	1	2	1	2	1	2
+/-/~	-	0/30/0	-	0/30/0	-	0/30/0	-	1/29/0	-	1/28/1	-	1/29/0
p-value	-	1.86E-09	-	1.86E-09	-	1.86E-09	-	2.24E-06	-	5.59E-09	-	5.59E-09

the  $\exp_{t+1}^k = \exp_t^k + 1$  update method (denoted as Fuzzy-UCS<sub>\*</sub>-NoMemb). Statistical results of the Wilcoxon signed-rank test are summarized with symbols wherein “+”, “-”, and “~” represent that the classification accuracy of Fuzzy-UCS<sub>\*</sub>-NoMemb is significantly better, worse, and competitive compared to that obtained by Fuzzy-UCS<sub>\*</sub>-Memb, respectively. The “*p*-value” is derived from the Wilcoxon signed-rank test. Arrows denote whether the rank improved or declined compared to Fuzzy-UCS<sub>\*</sub>-Memb. † indicates statistically significant differences compared to Fuzzy-UCS<sub>\*</sub>-Memb, i.e., *p*-value <  $\alpha = 0.05$ .

The experimental results indicate that Fuzzy-UCS<sub>\*</sub>-Memb achieved higher training and test accuracy compared to Fuzzy-UCS<sub>\*</sub>-NoMemb, as evidenced by lower average ranks in the table. The superior performance observed with the membership degree-based update method can be attributed to differentiated rule contribution in Fuzzy-UCS.

## C EXPERIMENTAL RESULTS ON STANDARD ACCURACY

This section presents the standard accuracy results for all systems. While macro F1 scores (presented in Section 6.2) provide a balanced measure accounting for both precision and recall, accuracy results are included here for comprehensive evaluation.

Tables 9 and 10 present each system’s average training and test classification accuracy and average rank across all datasets At the 10th and 50th epochs, respectively. Green-shaded values denote the best values among all systems, while peach-shaded values indicate the worst values among all systems. The terms “Rank” and “Position” denote each system’s overall average rank obtained by using the Friedman test and its position in the final ranking, respectively. Statistical results of the Wilcoxon signed-rank test are summarized with symbols wherein “+”, “-”, and “~” represent that the classification signed-rank accuracy of a conventional system is significantly better, worse, and competitive compared to that obtained by the proposed Fuzzy-UCS<sub>DS</sub>, respectively. The “ $p$ -value” and “ $p_{\text{Holm}}$ -value” are derived from the Wilcoxon signed-rank test and the Holm-adjusted Wilcoxon signed-rank test, respectively. Arrows denote whether the rank improved or declined compared to Fuzzy-UCS<sub>DS</sub>. † (††) indicates statistically significant differences compared to Fuzzy-UCS<sub>DS</sub>, i.e.,  $p$ -value ( $p_{\text{Holm}}$ -value)  $< \alpha = 0.05$ .

Table 9. Results When the Number of Training Iterations is 10 Epochs, Displaying Average Classification Accuracy Across 30 Runs.

10 Epochs	TRAINING ACCURACY (%)				TEST ACCURACY (%)			
	UCS	Fuzzy-UCS <sub>VOTE</sub>	Fuzzy-UCS <sub>SWIN</sub>	Fuzzy-UCS <sub>DS</sub>	UCS	Fuzzy-UCS <sub>VOTE</sub>	Fuzzy-UCS <sub>SWIN</sub>	Fuzzy-UCS <sub>DS</sub>
bnk	73.63 ~	89.60 ~	91.93 +	90.04	72.87 ~	89.20 ~	91.43 +	89.73
can	94.06 ~	93.91 ~	94.00 ~	94.03	90.23 ~	93.51 ~	93.63 ~	93.51
car	79.04 ~	83.33 ~	83.70 ~	84.37	70.00 ~	74.00 ~	77.33 ~	75.33
col	64.87 ~	69.33 +	67.14 ~	68.06	61.61 ~	66.56 ~	64.30 ~	65.27
dbt	69.81 ~	72.06 ~	70.97 ~	72.33	67.92 ~	69.09 ~	68.48 ~	69.18
ec1	65.14 ~	79.19 ~	75.93 ~	80.72	64.90 ~	79.71 ~	76.76 ~	80.98
frt	86.06 ~	83.02 ~	81.29 ~	85.78	81.00 ~	81.63 ~	79.85 ~	83.70
gls	54.32 ~	40.47 ~	61.60 ~	61.46	48.94 ~	36.36 ~	52.88 ~	52.88
hrt	83.24 ~	88.25 ~	89.58 ~	89.51	77.10 ~	81.94 ~	80.75 ~	82.47
hpt	85.11 +	76.24 ~	77.51 ~	77.10	57.92 ~	65.21 ~	64.38 ~	65.62
hc1	78.16 +	74.52 ~	73.95 ~	75.35	62.70 ~	68.29 ~	67.30 ~	68.74
irs	77.56 ~	93.68 ~	94.07 ~	94.35	74.67 ~	93.56 ~	94.22 ~	93.78
lnd	37.11 ~	27.71 ~	35.35 ~	43.34	32.16 ~	36.57 ~	35.69 ~	37.25
mam	79.79 ~	80.37 ~	77.59 ~	80.52	79.18 ~	78.76 ~	76.56 ~	79.04
pdy	72.47 +	50.43 ~	50.04 ~	52.40	71.57 +	50.93 ~	50.68 ~	53.06
pis	85.56 ~	86.66 ~	85.37 ~	86.64	84.42 ~	85.89 ~	84.26 ~	85.71
pha	76.45 ~	76.19 ~	78.60 +	77.40	59.75 ~	65.44 ~	62.89 ~	64.85
pre	99.33 ~	99.64 ~	100.0 +	99.61	99.34 ~	99.67 ~	100.0 +	99.60
pmp	86.45 ~	86.88 ~	86.45 ~	86.84	85.35 ~	86.19 ~	85.88 ~	86.24
rsn	80.33 ~	83.71 ~	85.16 +	84.38	81.74 ~	83.37 ~	85.11 +	84.37
seg	87.61 ~	88.93 ~	89.42 ~	89.26	87.30 ~	88.63 ~	89.16 ~	89.02
sir	71.81 ~	83.59 ~	83.96 ~	83.59	69.67 ~	81.00 ~	79.33 ~	81.00
smk	87.02 +	79.20 +	86.05 +	76.38	86.05 +	78.32 +	85.47 +	75.76
tae	53.75 ~	57.43 ~	60.64 ~	61.48	45.62 ~	49.79 ~	52.08 ~	53.75
tip	80.01 ~	80.34 ~	79.11 ~	80.40	78.69 ~	79.66 ~	77.97 ~	79.61
tit	70.05 +	69.28 ~	70.22 +	69.22	70.30 ~	68.89 ~	69.07 ~	68.56
wne	87.65 ~	97.12 ~	97.48 ~	97.56	84.44 ~	95.56 ~	94.63 ~	95.93
wbc	95.79 ~	96.47 ~	95.73 ~	96.63	94.90 ~	96.24 ~	94.38 ~	95.95
wpb	86.03 ~	86.89 ~	91.03 +	89.33	68.33 ~	75.17 ~	73.17 ~	75.17
yst	45.25 ~	45.91 ~	51.66 ~	54.14	42.10 ~	44.38 ~	50.74 ~	53.58
Rank	3.05↓††	2.75↓††	2.35↓	1.85	3.43↓††	2.25↓††	2.55↓††	1.77
Position	4	3	2	1	4	2	3	1
+/-/~	5/19/6	2/22/6	7/13/10	-	2/19/9	1/8/21	4/9/17	-
$p$ -value	0.00683	0.000479	0.120	-	0.000209	0.0143	0.00917	-
$p_{\text{Holm}}$ -value	0.0137	0.00144	0.120	-	0.000627	0.0183	0.0183	-

Table 10. Results When the Number of Training Iterations is 50 Epochs, Displaying Average Classification Accuracy Across 30 Runs.

50 Epochs	TRAINING ACCURACY (%)				TEST ACCURACY (%)			
	UCS	Fuzzy-UCS <sub>VOTE</sub>	Fuzzy-UCS <sub>SWIN</sub>	Fuzzy-UCS <sub>DS</sub>	UCS	Fuzzy-UCS <sub>VOTE</sub>	Fuzzy-UCS <sub>SWIN</sub>	Fuzzy-UCS <sub>DS</sub>
bnk	94.93 +	92.63 -	93.65 +	92.95	94.47 +	92.34 -	93.00 ~	92.63
can	97.19 +	95.29 -	94.83 -	95.39	91.75 -	94.74 ~	94.44 ~	94.80
car	81.56 -	87.93 ~	88.07 ~	88.22	71.33 ~	76.00 ~	76.67 ~	74.00
col	76.01 +	71.85 +	68.24 -	71.37	70.00 ~	69.35 ~	65.81 -	69.03
dbt	78.12 +	76.36 +	73.57 -	76.48	72.90 ~	73.07 ~	70.04 -	72.94
ec1	78.55 -	85.79 ~	80.39 -	85.64	76.18 -	84.02 ~	79.80 -	83.92
frt	93.67 +	87.12 -	85.17 -	88.43	83.41 -	84.74 -	82.33 -	86.44
gls	65.19 -	72.01 ~	71.75 ~	72.14	53.33 -	62.73 ~	64.09 ~	64.39
hrt	90.53 -	94.66 -	94.35 -	95.05	81.08 ~	81.83 ~	82.69 ~	81.83
hpt	90.10 -	91.46 -	89.88 -	92.33	57.08 -	64.58 ~	62.08 ~	65.62
hcl	89.86 +	87.25 -	84.19 -	87.76	63.69 -	71.80 ~	69.37 ~	71.62
irs	84.17 -	94.81 -	95.51 ~	95.26	81.78 -	94.00 ~	94.89 ~	94.22
lnd	55.29 +	32.05 -	39.18 -	46.27	42.06 ~	38.24 ~	40.10 ~	40.20
mam	83.10 +	80.89 -	77.89 -	81.07	80.72 ~	79.73 ~	76.77 -	80.03
pdy	89.16 +	50.94 -	50.70 -	53.94	88.24 +	51.46 ~	51.36 -	54.63
pis	87.54 +	86.89 ~	85.53 -	86.91	86.12 ~	85.88 ~	84.67 -	85.92
pha	79.17 -	82.10 -	86.80 +	85.64	62.55 -	66.96 ~	64.41 -	66.13
pre	99.63 ~	98.01 -	100.0 +	99.76	99.64 ~	98.03 -	100.0 +	99.79
pmp	87.24 ~	86.99 ~	86.89 -	87.03	86.01 ~	86.17 ~	86.05 ~	86.21
rsn	85.02 ~	84.33 -	85.51 +	85.13	84.63 ~	84.19 -	85.30 ~	85.07
seg	95.40 +	90.10 -	90.52 ~	90.42	93.02 +	89.88 -	90.01 ~	90.30
sir	76.96 -	84.78 ~	85.00 ~	84.78	70.67 -	81.67 ~	81.33 ~	82.00
smk	97.66 +	95.39 -	93.49 -	95.71	96.50 +	95.08 ~	93.14 -	95.11
tae	59.23 -	63.63 -	64.15 ~	64.35	49.17 -	54.58 ~	53.75 ~	56.46
tip	82.71 +	81.09 -	80.24 -	81.20	80.47 ~	80.00 -	78.88 -	80.23
tit	73.25 +	72.28 ~	70.57 -	72.38	72.30 ~	71.30 ~	68.93 -	71.52
wne	93.62 +	98.31 -	98.58 ~	98.79	88.52 -	96.48 ~	96.11 ~	96.67
wbc	97.59 +	97.12 ~	96.42 -	97.07	96.19 ~	96.19 ~	95.29 -	95.95
wpb	95.21 +	91.57 -	93.60 +	92.58	70.00 ~	72.17 ~	71.67 ~	72.00
yst	60.73 +	53.26 -	56.22 -	58.78	56.89 ~	52.04 -	53.65 -	57.61
Rank	2.10↓	2.98↓ <sup>††</sup>	2.93↓ <sup>††</sup>	1.98	2.72↓ <sup>††</sup>	2.50↓ <sup>††</sup>	2.93↓ <sup>††</sup>	1.85
Position	2	4	3	1	3	2	4	1
+/-/~	17/10/3	1/20/9	5/18/7	-	4/11/15	0/8/22	1/12/17	-
<i>p</i> -value	0.968	4.80E-05	0.00148	-	0.0483	0.0121	0.000529	-
<i>p</i> <sub>Holm</sub> -value	0.968	0.000144	0.00297	-	0.0483	0.0243	0.00159	-

Based on Tables 9 and 10, Fuzzy-UCS<sub>DS</sub> significantly outperformed all other systems ( $p_{\text{Holm}} < 0.05$ ) in test accuracy, securing the highest rank irrespective of the number of training epochs. In terms of training accuracy, Fuzzy-UCS<sub>DS</sub> also significantly outperformed all other systems ( $p_{\text{Holm}} < 0.05$ ), with the exception of Fuzzy-UCS<sub>SWIN</sub> at the 10th epoch and UCS at the 50th epoch, thereby achieving the highest rank. Furthermore, Tables 9 and 10 reveal that Fuzzy-UCS<sub>DS</sub> did not register the lowest accuracy for any problem regardless of the number of training epochs, except for the *smk* and *tit* problems in training and test accuracy at the 10th epoch. These findings underscore that Fuzzy-UCS<sub>DS</sub> is a robust system, consistently exhibiting high classification performance across a diverse range of problems.

## D EXPERIMENTS ON PROBLEMS WITH KNOWN GROUND TRUTH

While UCI and Kaggle datasets used in our experiment are invaluable for their diversity and ability to facilitate comparisons with existing work, they present limitations in terms of knowing inherent complexities and feature relevancies.

To mitigate the limitation of unknown ground truths in real-world datasets, we conduct supplementary experiments using artificial datasets where the underlying relationships and feature relevancies are predefined. Specifically, we utilize three artificial noiseless benchmark problems commonly employed in the LCS literature:

(1) *Real-Valued Multiplexer Problem*. The  $n$ -bit multiplexer problem ( $n$ -MUX) was initially introduced as a binary-valued classification problem to assess the generalization capability of XCS [Wilson 1995]. It was later extended for real-valued classification tasks [Aenugu and Spector 2019; Nakata and Browne 2021; Wilson 1999]. The  $n$ -MUX is tailored for binary strings defined by  $n = k + 2^k$ , where the initial  $k$  bits, when converted to decimal, correspond to one of the subsequent  $2^k$  bit positions. The correct class corresponds to the bit the first  $k$  bits indicate. In the real-valued version,  $n$ -RMUX, upon receiving an input  $\mathbf{x} \in [0, 1]^n$ , each attribute  $x_i$  is binarized using a threshold of 0.5 (i.e., 0 if  $x_i < 0.5$ , and 1 otherwise). The correct class for this real-valued input is ascertained using the same procedure applied to  $n$ -MUX. We use 11-RMUX, denoted as `mux`.

(2) *Real-Valued Majority-On Problem*. The  $n$ -bit majority-on problem ( $n$ -MAJ) was originally designed for binary-valued inputs [Iqbal et al. 2014]. In  $n$ -MAJ, the correct class is determined as 1 if the count of “1”s surpasses that of “0”s, and 0 otherwise. This article utilizes the recent extended version,  $n$ -RMAJ, tailored for real-valued classification [Hamasaki and Nakata 2021]. Similar to  $n$ -RMUX, each attribute  $x_i$  is binarized using the 0.5 threshold. The  $n$ -RMAJ is a highly overlapping problem and is known to suffer significantly from performance improvements in the hyperrectangular representation used in UCS. This article uses 11-RMAJ, denoted as `maj`.

(3) *Real-Valued Carry Problem*. The  $n$ -bit carry problem ( $n$ -CAR) was initially developed for binary-valued inputs [Iqbal et al. 2014]. In  $n$ -CAR, equal-length binary numbers are summed. Consequently, the output is 1 if there is a carry-over and 0 otherwise. For instance, with 3-bit numbers 101 and 001, the output stands at 0, while for 100 and 100, it is 1.  $n$ -CAR is an overlapping problem. This article extends  $n$ -CAR to a real-valued classification framework termed  $n$ -RCAR. Each attribute  $x_i$  is binarized using the 0.5 threshold, the same as in  $n$ -RMUX and  $n$ -RMAJ. This article uses 12-RCAR, denoted as `car`.

For all the artificial noiseless problems, each dataset consists of 6,000 data points uniformly sampled at random from the input space. The details of the datasets are shown in Table 11. The settings used in our experiments adhere to those outlined in Section 6.1. The number of training iterations is set to 10 and 50 epochs. To the best of our knowledge, there has been no comprehensive evaluation of the performance of LFCSs with linguistic rules, including Fuzzy-UCS, across all these problem domains. It is worth noting that these benchmark problems were originally designed for real-valued LCSs, such as XCSR and UCS, where the antecedent part of each rule is represented by a combination of lower and upper bounds for each dimension.

Tables 12 and 13 present each system’s average training and test classification accuracy and average rank across all datasets at the 10th and 50th epochs, respectively. Green-shaded values denote the best values among all systems, while peach-shaded values indicate the worst values among all systems. The terms “Rank” and “Position” denote each system’s overall average rank obtained by using the Friedman test and its position in the final ranking, respectively. Statistical results of the Wilcoxon signed-rank test are summarized with symbols wherein “+”, “-”, and “~” represent that the classification accuracy of a conventional system is significantly better, worse, and competitive compared to that obtained by the proposed Fuzzy-UCS<sub>DS</sub>, respectively. The “ $p$ -value” is

Table 11. Properties of the three Artificial Noiseless Datasets. The Columns Describe: the Identifier (ID.), the Name (Name), the Number of Instances (#INST.), the Total Number of Features (#FEA.), the Number of Classes (#CL.), the Percentage of Missing Attributes (%Mis.), the Percentage of Instances of the Majority Class (%MAJ.), the Percentage of Instances of the Minority Class (%MIN.), and the Source (Ref.).

ID.	Name	#INST.	#FEA.	#CL.	%Mis.	%MAJ.	%MIN.	Ref.
car	12 bit real-valued carry	6000	12	2	0	50.85	49.15	[Iqbal et al. 2014]
maj	11 bit real-valued majority-on	6000	11	2	0	50.22	49.78	[Hamasaki and Nakata 2021]
mux	11 bit real-valued multiplexer	6000	11	2	0	50.50	49.50	[Wilson 1999]

Table 12. Results When the Number of Training Iterations is 10 Epochs, Displaying Average Classification Accuracy Across 30 Runs.

10 Epochs	TRAINING ACCURACY (%)				TEST ACCURACY (%)			
	UCS	Fuzzy-UCS <sub>VOTE</sub>	Fuzzy-UCS <sub>SWIN</sub>	Fuzzy-UCS <sub>DS</sub>	UCS	Fuzzy-UCS <sub>VOTE</sub>	Fuzzy-UCS <sub>SWIN</sub>	Fuzzy-UCS <sub>DS</sub>
car	87.57 +	85.57 -	86.50 +	85.92	86.45 ~	85.74 ~	86.64 +	85.95
maj	83.64 -	85.72 -	86.04 -	86.34	81.84 -	85.54 -	85.31 -	86.23
mux	72.32 -	74.53 -	76.42 +	75.00	69.54 -	73.26 -	74.73 +	73.66
Rank	3.00↓	3.33↓	1.67↑	2.00	3.33↓	3.00↓	1.67↑	2.00
Position	3	4	1	2	4	3	1	2
+/-/~	1/2/0	0/3/0	2/1/0	-	0/2/1	0/2/1	2/1/0	-

Table 13. Results When the Number of Training Iterations is 50 Epochs, Displaying Average Classification Accuracy Across 30 Runs.

50 Epochs	TRAINING ACCURACY (%)				TEST ACCURACY (%)			
	UCS	Fuzzy-UCS <sub>VOTE</sub>	Fuzzy-UCS <sub>SWIN</sub>	Fuzzy-UCS <sub>DS</sub>	UCS	Fuzzy-UCS <sub>VOTE</sub>	Fuzzy-UCS <sub>SWIN</sub>	Fuzzy-UCS <sub>DS</sub>
car	93.89 +	86.50 -	88.22 +	86.99	92.28 +	86.43 -	88.08 +	86.87
maj	90.19 +	86.22 -	87.07 ~	86.90	87.23 ~	85.81 -	85.68 -	86.44
mux	93.02 +	86.50 ~	86.08 -	86.51	92.17 +	85.16 ~	84.87 ~	85.26
Rank	1.00↑	3.67↓	2.67	2.67	1.00↑	3.33↓	3.33↓	2.33
Position	1	4	2.5	2.5	1	3.5	3.5	2
+/-/~	3/0/0	0/2/1	1/1/1	-	2/0/1	0/2/1	1/1/1	-

derived from the Wilcoxon signed-rank test. Arrows denote whether the rank improved or declined compared to Fuzzy-UCS<sub>DS</sub>.

Based on Table 12, at the 10th epoch, Fuzzy-UCS<sub>SWIN</sub> achieved the highest rank in both training and testing. This suggests that single winner-based inference, which relies on the rule with the highest fitness, was effective for noiseless problems when training iterations were limited. Conversely, UCS recorded the lowest rank in testing at the 10th epoch. As discussed in Section 6.3.1, this is likely because the crisp rules used by UCS were not sufficiently optimized with limited training iterations. Indeed, when given sufficient training time (i.e., at the 50th epoch, cf. Table 13), UCS achieved the highest rank in both training and testing. This can be attributed to UCS's rule antecedent representation (i.e., unordered bound hyperrectangular representation) being more flexible than Fuzzy-UCS\*'s linguistic label representation, coupled with the noiseless nature of the problems solved.

It is noteworthy that in situations where rules were sufficiently optimized (i.e., at the 50th epoch), the proposed Fuzzy-UCS<sub>DS</sub> outperformed Fuzzy-UCS<sub>VOTE</sub> and Fuzzy-UCS<sub>SWIN</sub> in terms of test accuracy, as evidenced by the average rankings. Furthermore, Fuzzy-UCS<sub>DS</sub> never recorded the worst performance among all systems at both the 10th and 50th epochs (i.e., no peach-colored cells), leading to the conclusion that Fuzzy-UCS<sub>DS</sub> demonstrates stable performance regardless of the presence or absence of noise. Particularly, as shown in Appendix C, Fuzzy-UCS<sub>DS</sub> exhibits

high classification accuracy for real-world problems with high uncertainty, such as those involving noise.

In summary, the insights gained from experiments with artificial noiseless datasets can be summarized as follows:

- UCS, which uses non-linguistic crisp rules, records superior test accuracy compared to Fuzzy-UCS<sub>\*</sub> in noiseless problems. However, when training iterations are limited, its test accuracy is inferior to Fuzzy-UCS<sub>\*</sub> due to the higher difficulty of optimizing crisp rules.
- The single-winner-based inference (Fuzzy-UCS<sub>SWIN</sub>), which relies on the rule with the highest fitness, is often effective in noiseless problems.
- Fuzzy-UCS<sub>DS</sub> demonstrates stable performance regardless of the presence or absence of noise. Notably, it achieves high classification accuracy for real-world problems characterized by high uncertainty, including those involving noise.

## E SCALABILITY AND PERFORMANCE ON LARGER-SCALE DATASETS

To further validate our algorithm’s effectiveness and scalability, we extend our experiments to include larger and more complex datasets. These datasets, characterized by either a high number of features or instances, are detailed in Table 14. This expansion allows us to assess how well our proposed algorithm adapts to increased data volume and feature complexity, mirroring real-world challenges across various domains.

The settings used in our experiments adhere to those outlined in Section 6.1. The number of training iterations is set to 50 epochs. For datasets with a large number of features (60 or more), specifically con, lib, and mcd, the hyperparameter  $P_{\#}$  for both UCS and Fuzzy-UCS\* is set to 0.8 to mitigate the risk of cover-delete cycles [Butz et al. 2004], a common occurrence in high-dimensional input problems.

Tables 15 and 16 present each system’s average training and test classification accuracy and average rank across all datasets at the 10th and 50th epochs, respectively. “+”, “-”, “~”, “Rank”, “Position”, arrows, and green- and peach-shaded values should be interpreted as in Tables 12 and 13.

<sup>13</sup><https://www.kaggle.com/datasets/shilpiic/myocardial-infarction/data> (June 12, 2025)

Table 14. Properties of the Four Larger-Scale Real-World Datasets. “ID”, “Name”, “#INST.”, “#FEA.”, “#CL.”, “%Mis.”, “%MAJ.”, “%MIN.”, and “Ref.” Should be Interpreted as in Table 11. Numerical Values Characterizing “Larger-Scale” are Shown in Bold.

ID.	Name	#INST.	#FEA.	#CL.	%Mis.	%MAJ.	%MIN.	Ref.
con	Connectionist bench (sonar, mines vs. rocks)	208	<b>60</b>	2	0	53.37	46.63	[Dua and Graff 2017]
lib	Libras movement	360	<b>90</b>	15	0	6.67	6.67	[Dua and Graff 2017]
mcd	Myocardial_infarction	1700	<b>111</b>	8	8.47	84.06	0.71	<sup>13</sup>
phi	Phishing Websites	<b>11055</b>	30	2	0	55.69	44.31	[Dua and Graff 2017]

Table 15. Results When the Number of Training Iterations is 10 Epochs, Displaying Average Classification Accuracy Across 30 Runs.

10 Epochs	TRAINING ACCURACY (%)				TEST ACCURACY (%)			
	UCS	Fuzzy-UCS <sub>VOTE</sub>	Fuzzy-UCS <sub>SWIN</sub>	Fuzzy-UCS <sub>DS</sub>	UCS	Fuzzy-UCS <sub>VOTE</sub>	Fuzzy-UCS <sub>SWIN</sub>	Fuzzy-UCS <sub>DS</sub>
con	78.07 ~	89.13 ~	93.24 +	91.19	28.61 ~	68.15 ~	72.13 ~	70.09
lib	99.73 +	85.48 ~	87.93 ~	88.72	83.24 ~	84.94 ~	84.84 ~	85.35
mcd	93.76 +	85.18 ~	85.61 ~	87.06	76.99 ~	92.99 ~	93.09 ~	93.21
phi	80.19 ~	93.58 ~	93.81 ~	93.87	60.32 ~	74.13 ~	72.54 ~	74.60
Rank	2.50↓	3.50↓	2.25↓	1.75	4.00↓	2.50↓	2.25↓	1.25
Position	3	4	2	1	4	3	2	1
+/-/~	2/2/0	0/4/0	1/1/2	-	0/4/0	0/3/1	0/1/3	-

Table 16. Results When the Number of Training Iterations is 50 Epochs, Displaying Average Classification Accuracy Across 30 Runs.

50 Epochs	TRAINING ACCURACY (%)				TEST ACCURACY (%)			
	UCS	Fuzzy-UCS <sub>VOTE</sub>	Fuzzy-UCS <sub>SWIN</sub>	Fuzzy-UCS <sub>DS</sub>	UCS	Fuzzy-UCS <sub>VOTE</sub>	Fuzzy-UCS <sub>SWIN</sub>	Fuzzy-UCS <sub>DS</sub>
con	91.80 ~	91.84 ~	94.39 +	92.80	66.19 ~	76.67 ~	74.92 ~	77.14
lib	99.89 +	83.24 ~	85.29 ~	85.28	28.43 ~	65.65 ~	66.39 ~	67.13
mcd	93.80 +	85.68 ~	87.25 ~	87.67	83.25 ~	85.27 ~	85.00 ~	85.43
phi	80.34 ~	94.11 ~	95.00 ~	94.91	76.91 ~	93.70 ~	93.98 ~	94.21
Rank	2.50↓	3.50↓	1.75↑	2.25	4.00↓	2.50↓	2.50↓	1.00
Position	3	4	1	2	4	2.5	2.5	1
+/-/~	2/1/1	0/4/0	1/0/3	-	0/4/0	0/2/2	0/1/3	-

From Tables 15 and 16, Fuzzy-UCS<sub>DS</sub> recorded the highest rank in test accuracy at both 10 and 50 epochs. Furthermore, across all datasets, no instances were observed where Fuzzy-UCS<sub>DS</sub> had significantly worse test accuracy (denoted by “+”). Therefore, Fuzzy-UCS<sub>DS</sub> demonstrates good performance even on larger-scale datasets. On the other hand, UCS using crisp rules and Fuzzy-UCS<sub>SWIN</sub> relying solely on the rule with the highest fitness showed significant superiority during training but not during testing. This indicates a tendency to overfit training data as the dataset scale increases.

These results suggest that while UCS and Fuzzy-UCS<sub>SWIN</sub> may excel during training, they are prone to overfitting on larger-scale datasets. In contrast, Fuzzy-UCS<sub>DS</sub> maintains stable performance regardless of dataset size, demonstrating its robustness and scalability.

## F COMPARISON WITH A STATE-OF-THE-ART NONFUZZY LCS

To further evaluate our proposed algorithm’s performance against a state-of-the-art nonfuzzy LCS designed for noisy datasets, we conduct additional experiments comparing it with scikit-ExSTraCS [Urbanowicz and Moore 2015]<sup>14</sup>. This system is chosen due to its open-source availability and reputation as a robust nonfuzzy LCS capable of handling complex noisy datasets.

The problems and settings used in our experiments adhere to those outlined in Section 6.1. The number of training iterations is set to 10 and 50 epochs. For scikit-ExSTraCS, we use the default hyperparameter values. However, to ensure a fair comparison, we only adjust the hyperparameters common to both UCS and Fuzzy-UCS as follows: learning\_iterations = 10 or 50 Epochs,  $N = 2000$ , theta\_GA = 50, theta\_del = 50, theta\_sub = 50, theta\_sel = 0.4, do\_correct\_set\_subsumption = True, and rule\_compaction = None.

Tables 17 and 18 present each system’s average training and test classification accuracy and average rank across all datasets at the 10th and 50th epochs, respectively. Green-shaded values denote the best values among all systems, while peach-shaded values indicate the worst values among all systems. The terms “Rank” and “Position” denote each system’s overall average rank obtained by using the Friedman test and its position in the final ranking, respectively. Statistical results of the Wilcoxon signed-rank test are summarized with symbols wherein “+”, “-”, and “~” represent that the classification accuracy of a conventional system is significantly better, worse, and competitive compared to that obtained by the proposed Fuzzy-UCS<sub>DS</sub>, respectively. The “ $p$ -value” and “ $p_{Holm}$ -value” are derived from the Wilcoxon signed-rank test and the Holm-adjusted Wilcoxon signed-rank test, respectively. Arrows denote whether the rank improved or declined compared to

<sup>14</sup><https://github.com/UrbsLab/scikit-ExSTraCS/tree/master> (June 12, 2025)

Table 17. Results When the Number of Training Iterations is 10 Epochs, Displaying Average Classification Accuracy Across 30 Runs.

10 Epochs	TRAINING ACCURACY (%)					TEST ACCURACY (%)				
	scikit-ExSTraCS	UCS	Fuzzy-UCS <sub>VOTE</sub>	Fuzzy-UCS <sub>SWIN</sub>	Fuzzy-UCS <sub>DS</sub>	scikit-ExSTraCS	UCS	Fuzzy-UCS <sub>VOTE</sub>	Fuzzy-UCS <sub>SWIN</sub>	Fuzzy-UCS <sub>DS</sub>
bnk	95.44 +	73.63 ~	89.60 ~	91.93 +	90.04	94.93 +	72.87 ~	89.20 ~	91.43 +	89.73
can	94.30 ~	94.06 ~	93.91 ~	94.00 ~	94.03	93.51 ~	90.23 ~	93.51 ~	93.63 ~	93.51
car	81.11 ~	79.04 ~	83.33 ~	83.70 ~	84.37	69.33 ~	70.00 ~	74.00 ~	77.33 ~	75.33
col	76.73 +	64.87 ~	69.33 +	67.14 ~	68.06	73.55 +	61.61 ~	66.56 ~	64.30 ~	65.27
dbt	75.77 +	69.81 ~	72.06 ~	70.97 ~	72.33	73.38 +	67.92 ~	69.99 ~	68.48 ~	69.18
ecl	84.61 +	65.14 ~	79.19 ~	75.93 ~	80.72	83.04 ~	64.90 ~	79.71 ~	76.76 ~	80.98
frt	84.09 ~	86.06 ~	83.02 ~	81.29 ~	85.78	81.67 ~	81.00 ~	81.63 ~	79.85 ~	83.70
gls	64.93 +	54.32 ~	40.47 ~	61.60 ~	61.46	60.30 +	48.94 ~	36.36 ~	52.88 ~	52.88
hrt	84.77 ~	83.24 ~	88.25 ~	89.58 ~	89.51	83.12 ~	77.10 ~	81.94 ~	80.75 ~	82.47
hpt	71.39 ~	85.11 +	76.24 ~	77.51 ~	77.10	67.08 ~	57.92 ~	65.21 ~	64.38 ~	65.62
hcl	75.77 ~	78.16 +	74.52 ~	73.95 ~	75.55	73.24 ~	72.67 ~	68.29 ~	67.30 ~	68.74
irs	94.72 ~	77.56 ~	93.68 ~	94.07 ~	94.35	94.22 ~	74.67 ~	93.56 ~	94.22 ~	93.78
lnd	49.76 +	37.11 ~	27.71 ~	35.35 ~	43.34	40.78 +	32.16 ~	36.57 ~	35.69 ~	37.25
mam	82.71 +	79.79 ~	80.37 ~	77.59 ~	80.52	81.75 +	79.18 ~	78.76 ~	76.56 ~	79.04
pdv	78.52 +	72.47 +	50.43 ~	50.04 ~	52.40	77.91 +	71.57 +	50.93 ~	50.68 ~	53.06
pis	85.99 ~	85.56 ~	86.66 ~	85.37 ~	86.64	85.46 ~	84.42 ~	85.89 ~	84.26 ~	85.71
pha	69.79 ~	76.45 ~	76.19 ~	78.60 +	77.40	65.93 ~	59.75 ~	65.44 ~	62.89 ~	64.85
pre	88.70 ~	99.33 ~	99.64 ~	100.0 +	99.61	88.87 ~	99.34 ~	99.67 ~	100.0 +	99.60
rmp	87.12 +	86.45 ~	86.88 ~	86.45 ~	86.84	86.29 ~	85.35 ~	86.19 ~	85.88 ~	86.24
rsn	85.44 +	80.33 ~	83.71 ~	85.16 +	84.58	85.11 ~	81.74 ~	83.37 ~	85.11 +	84.37
seg	91.12 +	87.61 ~	88.93 ~	89.42 ~	89.26	90.81 +	87.30 ~	88.63 ~	89.16 ~	89.02
sir	82.07 ~	71.81 ~	83.59 ~	83.96 ~	83.59	80.67 ~	69.67 ~	81.00 ~	79.33 ~	81.00
smk	96.14 +	87.02 +	79.20 +	86.05 +	76.38	95.99 +	86.05 +	78.32 +	85.47 +	75.76
tae	59.93 ~	53.75 ~	57.43 ~	60.64 ~	61.48	51.25 ~	45.62 ~	49.79 ~	52.08 ~	53.75
tip	76.23 ~	80.01 ~	80.34 ~	79.11 ~	80.40	74.86 ~	78.69 ~	79.66 ~	77.97 ~	79.61
tit	72.05 +	70.05 +	69.28 ~	70.22 +	69.22	71.30 +	70.30 ~	68.89 ~	69.07 ~	68.56
wne	95.77 ~	87.65 ~	97.12 ~	97.48 ~	97.56	93.33 ~	84.44 ~	95.56 ~	94.63 ~	95.93
wbc	97.63 +	95.79 ~	96.47 ~	95.73 ~	96.63	96.95 +	94.90 ~	96.24 ~	94.38 ~	95.95
wpb	71.44 ~	86.03 ~	86.89 ~	91.03 +	89.33	61.83 ~	68.33 ~	75.17 ~	73.17 ~	75.17
yst	59.91 +	45.25 ~	45.91 ~	51.66 ~	54.14	58.84 +	42.10 ~	44.38 ~	50.74 ~	53.58
Rank	2.30↑	3.82↑ <sup>††</sup>	3.42↑ <sup>††</sup>	3.02↓	2.45	1.97↑	4.30↑ <sup>††</sup>	3.00↑ <sup>††</sup>	3.28↑ <sup>††</sup>	2.45
Position	1	5	4	3	2	1	5	3	4	2
+/-/~	15/10/5	5/19/6	2/22/6	7/12/11	-	12/4/14	2/20/8	1/8/21	4/9/17	-
$p$ -value	0.503	0.00683	0.000479	0.120	-	0.0920	0.000209	0.0143	0.00917	-
$p_{Holm}$ -value	0.503	0.0205	0.00192	0.241	-	0.0920	0.000837	0.0285	0.0275	-

Table 18. Results When the Number of Training Iterations is 50 Epochs, Displaying Average Classification Accuracy Across 30 Runs.

50 Epochs	TRAINING ACCURACY (%)					TEST ACCURACY (%)				
	scikit-ExSTraCS	UCS	Fuzzy-UCS <sub>VOTE</sub>	Fuzzy-UCS <sub>SWIN</sub>	Fuzzy-UCS <sub>DS</sub>	scikit-ExSTraCS	UCS	Fuzzy-UCS <sub>VOTE</sub>	Fuzzy-UCS <sub>SWIN</sub>	Fuzzy-UCS <sub>DS</sub>
bnk	97.26 +	94.93 +	92.63 -	93.65 +	92.95	97.08 +	94.47 +	92.34 -	93.00 ~	92.63
can	95.48 ~	97.19 +	95.29 -	94.83 +	95.39	94.68 ~	91.75 -	94.74 ~	94.44 ~	94.80
car	86.15 -	81.56 -	87.93 ~	88.07 ~	88.22	75.33 ~	71.33 ~	76.00 ~	76.67 ~	74.00
col	80.91 +	76.01 +	71.85 +	68.24 -	71.37	77.31 +	70.00 ~	69.35 ~	65.81 -	69.03
dbt	78.09 +	78.12 +	76.36 ~	73.57 -	76.48	74.68 ~	72.90 ~	73.07 ~	70.04 ~	72.94
ecl	89.58 +	78.55 -	85.79 ~	80.39 -	85.64	86.47 +	76.18 -	84.02 ~	79.80 ~	83.92
frt	90.58 +	93.67 +	87.12 -	85.17 -	88.43	87.52 ~	83.41 -	84.74 -	82.33 -	86.44
gls	76.96 +	65.19 -	72.01 -	71.75 ~	72.14	65.30 ~	53.33 -	62.73 ~	64.09 ~	64.39
hrt	87.98 ~	90.53 ~	94.66 ~	94.35 ~	95.05	83.98 ~	81.08 ~	81.83 ~	82.69 ~	81.83
hpt	75.56 -	90.10 ~	91.46 ~	89.88 ~	92.33	68.12 ~	57.08 -	64.58 ~	62.08 ~	65.62
hcl	81.85 -	89.86 +	87.25 ~	84.19 -	87.76	76.22 +	63.69 -	71.80 ~	69.37 ~	71.62
irs	96.57 +	84.17 -	94.81 ~	95.51 ~	95.26	94.00 ~	81.78 -	94.00 ~	94.89 ~	94.22
lnd	61.85 +	55.29 +	32.05 -	39.18 -	46.27	47.94 +	42.06 ~	38.24 ~	40.10 ~	40.20
mam	83.00 +	83.10 +	80.89 ~	77.89 -	81.07	81.75 +	80.72 ~	79.73 ~	76.77 ~	80.03
pdv	80.14 +	89.16 +	50.94 -	50.70 -	53.94	79.51 +	88.24 +	51.46 ~	51.36 ~	54.63
pis	86.69 ~	87.54 +	86.89 ~	85.53 -	86.91	85.91 ~	86.12 ~	85.88 ~	84.67 ~	85.92
pha	76.79 ~	79.17 ~	82.10 ~	86.80 +	85.64	65.83 ~	62.55 ~	66.96 +	64.41 ~	66.13
pre	88.61 -	99.63 +	98.01 ~	100.0 +	99.76	89.00 ~	99.64 ~	98.03 ~	100.0 +	99.79
pmp	87.69 +	87.24 ~	86.99 ~	86.89 ~	87.03	86.84 +	86.01 ~	86.17 ~	86.05 ~	86.21
rsn	86.15 +	85.02 ~	84.33 ~	85.51 +	85.13	86.00 +	84.63 ~	84.19 ~	85.30 ~	85.07
seg	94.34 +	95.40 +	90.10 ~	90.52 ~	90.42	93.82 +	93.02 +	89.88 ~	90.01 ~	92.00
sir	87.22 +	76.96 ~	84.78 ~	85.00 ~	84.78	82.33 ~	70.67 ~	81.67 ~	81.33 ~	83.30
smk	98.67 +	97.66 +	95.39 ~	93.49 -	95.71	98.87 +	96.5 +	95.08 ~	93.14 -	95.11
tae	67.83 +	59.23 ~	63.63 ~	64.15 ~	64.35	52.29 ~	49.17 ~	54.58 ~	53.75 ~	56.46
tip	80.39 ~	82.71 +	81.09 ~	80.24 ~	81.20	77.87 ~	80.47 ~	80.00 ~	78.88 ~	80.23
tit	74.04 +	73.25 +	72.28 ~	70.57 ~	72.38	72.56 ~	72.30 ~	71.30 ~	68.93 ~	71.52
wne	98.40 ~	93.62 ~	98.31 ~	98.58 ~	98.79	95.19 ~	88.52 ~	96.48 ~	96.11 ~	96.67
wbc	97.90 +	97.59 +	97.12 ~	96.42 ~	97.07	96.57 ~	96.19 ~	96.19 ~	95.29 ~	95.95
wpb	77.13 -	95.21 +	91.57 ~	93.60 +	92.58	64.83 ~	70.00 ~	72.17 ~	71.67 ~	72.00
yst	63.19 +	60.73 +	53.26 -	56.22 ~	58.78	59.66 +	56.89 ~	52.04 ~	53.65 ~	57.61
Rank	2.37 <sup>†</sup>	2.63 <sup>††</sup>	3.68 <sup>†††</sup>	3.67 <sup>†††</sup>	2.65	1.98 <sup>†††</sup>	3.55 <sup>†††</sup>	3.22 <sup>†††</sup>	3.70 <sup>†††</sup>	2.55
Position	1	2	5	4	3	1	3	5	2	2
+/-/~	19/9/2	17/10/3	1/20/9	5/18/7	-	12/3/15	4/11/15	1/8/21	1/11/18	-
p-value	0.229	0.968	4.80E-05	0.00148	-	0.0185	0.0483	0.0121	0.000529	-
$p_{Holm}$ -value	0.457	0.968	0.000192	0.00445	-	0.0371	0.0483	0.0364	0.00211	-

Fuzzy-UCS<sub>DS</sub>. † (††) indicates statistically significant differences compared to Fuzzy-UCS<sub>DS</sub>, i.e.,  $p$ -value ( $p_{Holm}$ -value)  $< \alpha = 0.05$ .

From Tables 17 and 18, scikit-ExSTraCS recorded the highest rank in test accuracy at both the 10th and 50th epochs. Particularly at the 50th epoch, Fuzzy-UCS<sub>DS</sub> performed significantly worse than scikit-ExSTraCS ( $p_{Holm} = 0.0371$ ). However, it is crucial to interpret these results in the context of the fundamental differences between the two systems:

- Fuzzy-UCS is a “fuzzified” version of UCS, designed as a simple and fundamental system.
- In contrast, scikit-ExSTraCS incorporates several specialized mechanisms specifically designed for noisy datasets, including:
  - Attribute Feedback: Guides rule generalization based on attribute tracking scores.
  - Attribute Tracking: Tracks attribute importance for each training instance.
  - Mixed Discrete-Continuous Attribute List Knowledge Representation: Efficiently handles both discrete and continuous attributes compared to linguistic terms.

Given these architectural differences, the performance gap is not unexpected and highlights the trade-offs between simplicity and specialized optimization.

Additionally, Table 19 shows UCS, Fuzzy-UCS\*, and scikit-ExSTraCS’s average macro-ruleset size and average rank across all datasets at the 10th and 50th epochs, respectively. Green-shaded values denote the best (smallest) values among all systems, while peach-shaded values indicate the worst (largest) values among all systems. Statistical results of the Wilcoxon signed-rank test are summarized with symbols wherein “+”, “-”, and “~” represent that the macro-ruleset size of a conventional system is significantly smaller, larger, and competitive compared to that obtained by Fuzzy-UCS\*, respectively. Arrows denote whether the rank improved or declined compared

Table 19. Results Displaying Average Macro-Ruleset Size Across 30 Runs.

	MACRO-RULESET SIZE					
	10 Epochs			50 Epochs		
	scikit-ExSTraCS	UCS	Fuzzy-UCS <sub>*</sub>	scikit-ExSTraCS	UCS	Fuzzy-UCS <sub>*</sub>
bnk	1335 –	811.0 –	642.9	1536 –	1285 –	1244
can	579.3 +	1609 –	1081	1702 +	1750 ~	1744
car	47.87 +	44.57 +	70.83	94.60 +	218.8 +	257.7
col	432.3 –	256.9 ~	274.4	1670 –	1275 –	1084
dbt	1247 –	942.4 ~	894.2	1790 –	1584 –	1546
ecl	746.3 –	461.8 ~	485.7	1694 –	1467 –	1357
frr	1796 +	1817 ~	1811	1824 +	1826 +	1858
gls	589.4 –	374.5 +	543.0	1826 –	1430 –	1313
hrt	453.6 +	968.5 +	1429	1667 –	1622 ~	1620
hpt	213.9 +	920.2 +	1019	1228 +	1683 ~	1690
hcl	392.2 +	1648 ~	1646	1561 +	1777 ~	1786
irs	152.9 –	78.50 +	88.50	574.1 –	477.2 –	357.4
lnd	941.9 –	411.1 –	349.9	1579 –	1374 –	723.0
mam	1117 –	832.0 –	705.5	1294 +	1478 –	1412
pdv	1634 –	1420 –	846.8	1581 –	1403 –	912.4
pis	1777 –	1653 –	1629	1727 –	1668 +	1704
pha	1114 +	1604 +	1678	1772 –	1692 +	1725
pre	1687 –	1194 –	870.1	1723 –	958.1 ~	990.4
pmp	1751 –	1608 –	1544	1682 ~	1630 +	1669
rsn	883.0 –	722.5 –	540.3	1601 –	1512 –	1464
seg	1783 –	1693 +	1712	1736 –	1701 ~	1709
sir	148.6 –	77.37 +	120.9	586.3 –	444.0 ~	441.1
smk	503.7 +	748.4 –	618.0	1465 ~	1425 +	1482
tae	302.5 –	188.6 +	264.2	1521 –	1073 –	907.5
tip	1679 –	1633 ~	1621	1665 –	1569 +	1615
tit	1112 +	826.8 +	1233	1521 ~	1538 ~	1521
wne	323.1 +	355.7 ~	349.8	1623 –	1396 –	1340
wbc	738.7 +	1223 –	1171	1036 +	1538 –	1527
wpb	271.9 +	1502 –	1021	1655 +	1826 –	1782
yst	1873 –	1586 –	1264	1832 –	1632 –	1548
Rank	2.27↓	1.93↓	1.80	2.38↓††	1.93↓††	1.68
Position	3	2	1	3	2	1
+/-/~	12/18/0	10/13/7	-	8/19/3	7/15/8	-
<i>p</i> -value	0.490	0.221	-	0.0195	0.0262	-
<i>p</i> <sub>Holm</sub> -value	0.490	0.441	-	0.0390	0.0390	-

to Fuzzy-UCS<sub>\*</sub>. † (††) indicates statistically significant differences compared to Fuzzy-UCS<sub>\*</sub>, i.e., *p*-value (*p*<sub>Holm</sub>-value) <  $\alpha = 0.05$ . “Rank” and “Position” should be interpreted as in Tables 17 and 18.

Table 19 reveals that Fuzzy-UCS<sub>\*</sub> achieved the highest average rank (best among all methods) in terms of ruleset size at both the 10th and 50th epochs, while scikit-ExSTraCS recorded the third-best rank (worst among all methods). Notably, at the 50th epoch, Fuzzy-UCS<sub>\*</sub> generated significantly fewer rules compared to both UCS and scikit-ExSTraCS (*p*<sub>Holm</sub> = 0.0390). This finding aligns with previous research [Orriols-Puig et al. 2009], which suggests that the linguistic rule representation inherent in fuzzy rules (used in Fuzzy-UCS<sub>\*</sub>) promotes better rule generalization compared to non-linguistic rules (used in UCS and scikit-ExSTraCS). Specifically, the use of linguistic terms in fuzzy rules enhances the system’s ability to capture and represent knowledge in a more general form.

Given that scikit-ExSTraCS achieved higher test accuracy than Fuzzy-UCS<sub>\*</sub> at both the 10th and 50th epochs, these findings demonstrate an important trade-off: while scikit-ExSTraCS achieves higher test accuracy, it does so with more complex non-linguistic rule representations and a larger number of rules compared to Fuzzy-UCS<sub>\*</sub>’s interpretable linguistic rules. These results highlight the trade-off between complexity and classification performance.

For future research directions, we are considering several ways:

- (1) Enhancing Fuzzy-UCS<sub>DS</sub> by selectively incorporating some of scikit-ExSTraCS's noise-handling mechanisms while maintaining its core simplicity and interoperability.
- (2) Exploring the integration of fuzzy rule representations into scikit-ExSTraCS or adapting its inference scheme to incorporate the DS theory, potentially leading to a powerful hybrid approach that combines the strengths of both Fuzzy-UCS<sub>DS</sub> and scikit-ExSTraCS.
- (3) A comprehensive review and improvement of the entire Fuzzy-UCS framework. While our current research focused primarily on the decision-making mechanism (i.e., test phase), we recognize that there is significant room for improvement in the rule production mechanism (i.e., training phase).

In conclusion, while our current approach demonstrates the effectiveness of incorporating DS theory into the decision-making process of Fuzzy-UCS, there is still considerable room for improvement in other aspects of the system. Future work will aim to address these challenges, potentially leading to a more robust and versatile LFCS framework capable of handling complex, noisy datasets while maintaining high interpretability.

## G COMPARISON WITH STATE-OF-THE-ART CLASSIFICATION METHODS

To further evaluate our proposed algorithm's performance against more advanced classification methods, we conduct additional experiments using Random Forest [Breiman 2001] and XGBoost [Chen and Guestrin 2016]. These systems are chosen due to their widespread recognition as state-of-the-art methods for handling complex datasets effectively.

The experimental setup follows the conditions outlined in Section 6. We use standard implementations of Random Forest<sup>15</sup> and XGBoost<sup>16</sup>, ensuring consistent dataset splits for fair comparison. For Random Forest and XGBoost, we use default hyperparameter settings. For UCS and Fuzzy-UCS\*, the number of training iterations is set to 50 epochs.

Table 20 presents each system's average training and test classification accuracy, respectively, and average rank across all datasets. "+", "-", "~", "Rank", "Position", arrows, "†(††)", "p-value", "p<sub>Holm</sub>-value", and green- and peach-shaded values should be interpreted as in Tables 17 and 18.

From Table 20, Random Forest, XGBoost, and Fuzzy-UCS<sub>DS</sub> ranked first, second, and third in average rank during both training and testing phases. Notably, during training, Random Forest and XGBoost achieved 100% classification accuracy on many datasets.

These results highlight the fundamental differences in design philosophy between these approaches. Random Forest and XGBoost are ensemble learning techniques that aggregate multiple complex decision trees, excelling in capturing intricate patterns within data. In contrast, Fuzzy-UCS\* (an LFCS) is designed to prioritize interpretability through the use of fuzzy rules with easy-to-understand linguistic terms.

A recent survey on explainable artificial intelligence (XAI) [Ortigossa et al. 2024] emphasizes that while methods like Random Forest and XGBoost offer superior learning performance compared to rule-based systems (including LFCSs), they provide significantly lower model interpretability. This

<sup>15</sup><https://scikit-learn.org/dev/modules/generated/sklearn.ensemble.RandomForestClassifier.html> (June 12, 2025)

<sup>16</sup><https://xgboost.readthedocs.io/en/stable/python/index.html> (June 12, 2025)

Table 20. Results Displaying Average Classification Accuracy Across 30 Runs.

	TRAINING ACCURACY (%)						TEST ACCURACY (%)					
	Random Forest	XGBoost	UCS	Fuzzy-UCS <sub>VOTE</sub>	Fuzzy-UCS <sub>SWIN</sub>	Fuzzy-UCS <sub>DS</sub>	Random Forest	XGBoost	UCS	Fuzzy-UCS <sub>VOTE</sub>	Fuzzy-UCS <sub>SWIN</sub>	Fuzzy-UCS <sub>DS</sub>
bnk	100.0+	100.0+	94.93+	92.63-	93.65+	92.95	99.47+	99.28+	94.47+	92.34-	93.00-	92.63
can	100.0+	100.0+	97.19+	95.29-	94.83-	95.39	95.85-	96.67+	91.75-	94.74-	94.44-	94.80
car	90.22+	90.15+	81.56-	87.93-	88.07-	88.22	77.33~	75.33~	71.33~	76.00-	76.67-	74.00
col	100.0+	100.0+	76.01+	71.85+	68.24-	71.37	84.62+	84.62+	70.00-	69.35-	65.81-	69.03
dbt	100.0+	100.0+	78.12+	76.36-	73.57-	76.48	75.71+	72.73-	72.90-	73.07-	70.04-	72.94
ecl	100.0+	100.0+	78.55-	85.79-	80.39-	85.64	89.22+	86.47+	76.18-	84.02-	79.80-	83.92
frt	100.0+	100.0+	93.67+	87.12-	85.17-	88.43	90.04+	91.37+	83.41-	84.74-	82.33-	86.44
gls	100.0+	100.0+	65.19-	72.01-	71.75-	72.14	79.55+	77.88+	53.33-	62.73-	64.09-	64.39
hrt	100.0+	100.0+	90.53-	94.66-	94.35-	95.05	83.55-	80.32-	81.08-	81.83-	82.69-	81.83
hpt	99.98+	100.0+	90.10-	91.46-	89.88-	92.33	67.50-	60.62-	57.08-	64.58-	62.08-	65.62
hcl	100.0+	100.0+	89.86+	87.25-	84.19-	87.76	86.40+	86.31+	63.69-	71.80-	69.37-	71.62
irs	99.98+	100.0+	84.17-	94.81-	95.51-	95.26	94.89~	94.00~	81.78-	94.00-	94.89~	94.22
lnd	100.0+	100.0+	55.29+	32.05-	39.18-	46.27	50.78+	58.92+	42.06-	38.24-	40.10-	40.20
nam	94.79+	93.08+	83.10+	80.89-	77.89-	81.07	79.18~	78.83~	80.72~	79.73~	76.77~	80.03
pdy	100.0+	99.95+	89.16+	50.94-	50.70-	53.94	95.37+	94.91+	88.24+	51.46-	51.36-	54.63
pis	99.99+	100.0+	87.54+	86.89-	85.53-	86.91	86.90+	86.79+	86.12~	85.88-	84.67-	85.92
pha	99.99+	99.93+	79.17-	82.10-	86.80+	85.64	65.64~	63.48~	62.55~	66.96+	64.41-	66.13
pre	100.0+	100.0+	99.63~	98.01-	100.0+	99.76	100.0+	100.0+	99.64~	98.03~	100.0+	99.79
pmp	99.99+	99.97+	87.24~	86.99-	86.89-	87.03	88.39+	87.57+	86.01-	86.17-	86.05-	86.21
rsn	100.0+	99.89+	85.02~	84.33-	85.51+	85.13	86.48+	86.07+	84.63~	84.19-	85.30-	85.07
seg	100.0+	100.0+	95.40+	90.10-	90.52-	90.42	98.31+	98.67+	93.02+	89.88-	90.01-	90.30
sir	100.0+	100.0+	76.96-	84.78-	85.00-	84.78	85.33~	83.33~	70.67-	81.67-	81.33~	82.00
smk	100.0+	99.99+	97.66+	95.39-	93.49-	95.71	99.29+	99.26+	96.50+	95.08-	93.14-	95.11
tae	96.91+	96.37+	59.23~	63.60-	64.15-	64.35	66.88+	65.00+	49.17-	54.58-	53.75-	56.46
tip	91.85+	89.64+	82.71+	81.09-	80.24-	81.20	79.53~	80.35~	82.40~	80.00-	78.88-	80.23
tit	95.93+	93.28+	73.25~	72.28-	70.57-	72.38	70.81~	69.96~	70.37~	71.30~	68.93~	71.52
wne	100.0+	100.0+	93.62-	98.31-	98.58-	98.79	98.15~	96.48~	88.52-	96.48~	96.11~	96.67
wbc	100.0+	100.0+	97.59+	97.12-	96.42-	97.07	96.67+	95.29-	96.12~	96.19-	95.29~	95.95
wpb	100.0+	100.0+	95.21+	91.57-	93.60+	92.58	79.50+	81.17+	70.00-	72.17~	71.67~	72.00
yst	100.0+	99.86+	60.73+	53.26-	56.22-	58.78	62.80+	59.60+	56.89~	52.04-	53.65-	57.61
Rank	1.38††	1.65††	4.10†	4.98††	4.90††	3.98	1.63††	2.77††	4.42††	4.07††	4.70††	3.42
Position	1	2	4	5	6	3	1	2	6	4	5	3
+/-/~	30/0/0	30/0/0	17/10/3	1/20/9	5/18/7	-	19/0/11	18/1/11	4/11/15	1/8/21	1/11/18	-
p-value	1.86E-09	1.86E-09	0.968	4.80E-05	0.00148	-	1.07E-05	0.00385	0.0483	0.0121	0.000529	-
p <sub>Holm</sub> -value	9.31E-09	9.31E-09	0.968	0.000144	0.00297	-	5.37E-05	0.0116	0.0483	0.0243	0.00211	-

Table 21. Results Displaying Average Model Complexity Across 30 Runs. The columns Describe: Number of Trees per Model (#TREES), Average Depth per Tree (DEPTH), Number of Nodes per Model (#NODES) for Random Forest and XGBoost; and Number of Macro-Rules (#MACRO-RULES) for UCS and Fuzzy-UCS\*.

	Random Forest			XGBoost			UCS	Fuzzy-UCS*
	#TREES	DEPTH	#NODES	#TREES	DEPTH	#NODES	#MACRO-RULES	
bnk	100	8.2	5144	100	2.3	800	1285	1244
can	100	7.3	3872	100	2.0	646	1750	1744
car	100	5.3	2181	100	2.2	599	219	258
col	100	10.2	6770	300	3.3	3279	1275	1084
dbt	100	15.2	23688	100	6.0	3400	1584	1546
ecl	100	11.0	9637	800	2.1	5291	1467	1357
frt	100	12.4	13842	700	2.3	5501	1826	1858
gls	100	10.6	7554	600	2.2	4114	1430	1313
hrt	100	10.1	9402	100	4.3	1677	1622	1620
hpt	100	11.1	6544	100	4.0	1282	1683	1690
hcl	100	10.8	8860	100	3.9	1367	1777	1786
irs	100	5.2	1554	300	1.3	1138	477	357
lnd	100	13.7	24562	500	5.6	11724	1374	723
mam	100	17.7	31553	100	6.0	3510	1478	1412
pdy	100	19.6	105739	400	6.0	18517	1403	912
pis	100	16.0	33351	100	6.0	4178	1668	1704
pha	100	20.0	36535	100	6.0	3959	1692	1725
pre	100	10.1	9681	300	0.6	793	958	990
pmp	100	19.4	38273	100	6.0	3994	1630	1669
rsn	100	15.1	16520	100	6.0	2865	1512	1464
seg	100	14.8	17913	700	2.2	5582	1701	1709
sir	100	6.2	2280	100	2.1	574	444	441
smk	100	7.6	3527	100	2.5	712	1425	1482
tae	100	12.0	9248	300	5.4	5969	1073	908
tip	100	20.1	78694	100	6.0	5626	1569	1615
tit	100	19.8	39364	100	6.0	3601	1538	1521
wne	100	5.2	2068	300	0.6	785	1396	1340
wbc	100	9.1	5666	100	3.8	1098	1538	1527
wpb	100	8.8	4820	100	2.9	887	1826	1782
yst	100	24.0	83275	1000	4.8	25418	1632	1548
Average	100	12.6	21404	267	3.8	4296	1408	1344

underscores the trade-off between performance and interpretability in machine learning models. Table 21 presents a quantitative comparison of model complexity across different methods:

- Random Forest generated an average of 100 trees per model, with an average depth of 12.6 per tree, resulting in an average of 21,404 decision nodes per model.
- XGBoost generated an average of 267 trees per model, with an average depth of 3.8 per tree, resulting in an average of 4,296 decision nodes per model.
- UCS generated an average of 1,408 non-linguistic macro-rules.
- Fuzzy-UCS\* generated an average of 1,344 linguistic macro-rules.

This comparison demonstrates that while Random Forest and XGBoost achieve generally better performance, they lead to significantly higher model complexity. The linguistic rules in Fuzzy-UCS\* provide interpretable decision-making with good performance while maintaining lower model complexity.

Thus, our proposed Fuzzy-UCS<sub>DS</sub> system strikes a balance between these competing objectives. While it may not achieve the same classification accuracy as Random Forest or XGBoost on some datasets, it offers enhanced interpretability and the ability to quantify uncertainty. These features

are crucial in scenarios where understanding the decision-making process is as important as the final classification result.

It is important to emphasize that the primary contribution of our work is the improvement of the decision-making mechanism in LFCSs. By incorporating the DS theory-based class inference scheme, we enhanced the ability of LFCSs to handle uncertainty and provide more robust classifications, all while maintaining the interpretability that is a characteristic of these systems.

These findings highlight the trade-off between interpretability and classification performance. While Fuzzy-UCS<sub>DS</sub> may not outperform Random Forest or XGBoost in classification accuracy, it offers unique advantages in managing uncertainty and providing interpretable results. This makes it particularly valuable in domains where decision transparency is crucial, such as healthcare or finance. Future work includes the proposed DS theory-based class inference scheme with established methods like Random Forest and XGBoost, which could further enhance its performance across diverse datasets.

Received 3 June 2024; revised 22 October 2024, 5 February 2025; accepted 9 February 2025